I Strange matter: from strange nuggets to strange stars

II Explosive phenomena: burning of hadronic stars, compact stars merger and gamma-ray-bursts

Giuseppe Pagliara

Dipartimento di Fisica e Scienze della Terra, Universita' di Ferrara & INFN Ferrara, Italy

Helmholtz international summer school:
Nuclear theory and astrophysical applications
Dubna 10-22/07/2017

Collaborators

A. Drago, N. Dondi (Ferrara)

A. Lavagno (Torino)

G. Wiktorowicz (Varsaw)

S. Popov (Lomonosov, Moscow)

N. Bucciantini and A. Pili (Firenze)

Outline

-) Absolute stability of strange quark matter and strangelets pollution

-) Hadronic stars and strange stars in co-existence

-) Conversion of hadronic stars and connection with explosive phenomena

-) Testing the existence of strange stars through mergers (GW and shortGRBs)

Strange quark matter hypothesis

(Bodmer 71- Terazawa 79 - Witten 84)

Hyp: "three flavor beta-stable quark matter is more bound than ^{56}Fe."

Consider three massless quarks: up, down strange. From beta stability the chemical potentials $\mu_d = \mu_s$ implying that the density of strange = density of down. From charge neutrality then the number of up must be = to the number of down. The EoS:

$$P^f = \frac{\nu_f}{24\pi^2}\,(\mu^f)^4 = \frac{1}{3}\,\epsilon^f\,, \quad \rho^f = \frac{\nu_f}{6\pi^2}\,(\mu^f)^3$$

$$P = (\epsilon - 4B)/3\,.$$

Where ν_f=6 (color * spin degeneracy)
B is the bag constant of the MIT bag model

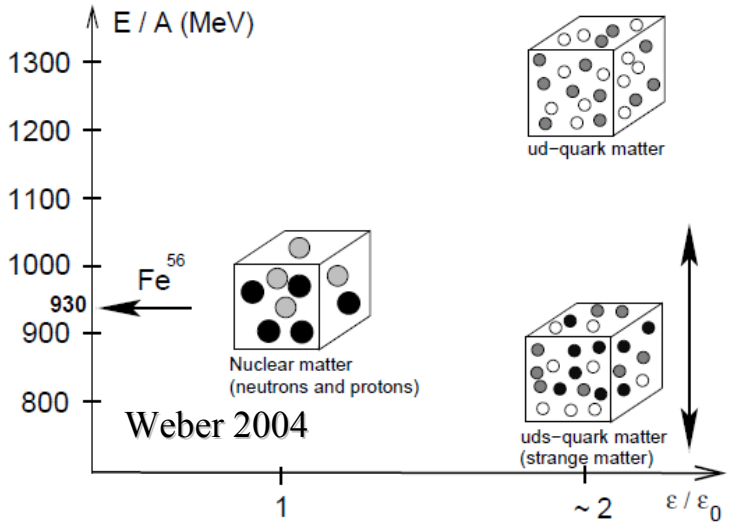

Starting with a mixture of up and down quarks, the weak process u+d->u+s allows to decrease E/A (a new Fermi sphere opens up) to values smaller than 930 MeV (depending on the values of the parameters!!!)

Varying the mass of the strange quark, the bag constant, the strength of perturbative QCD interactions.

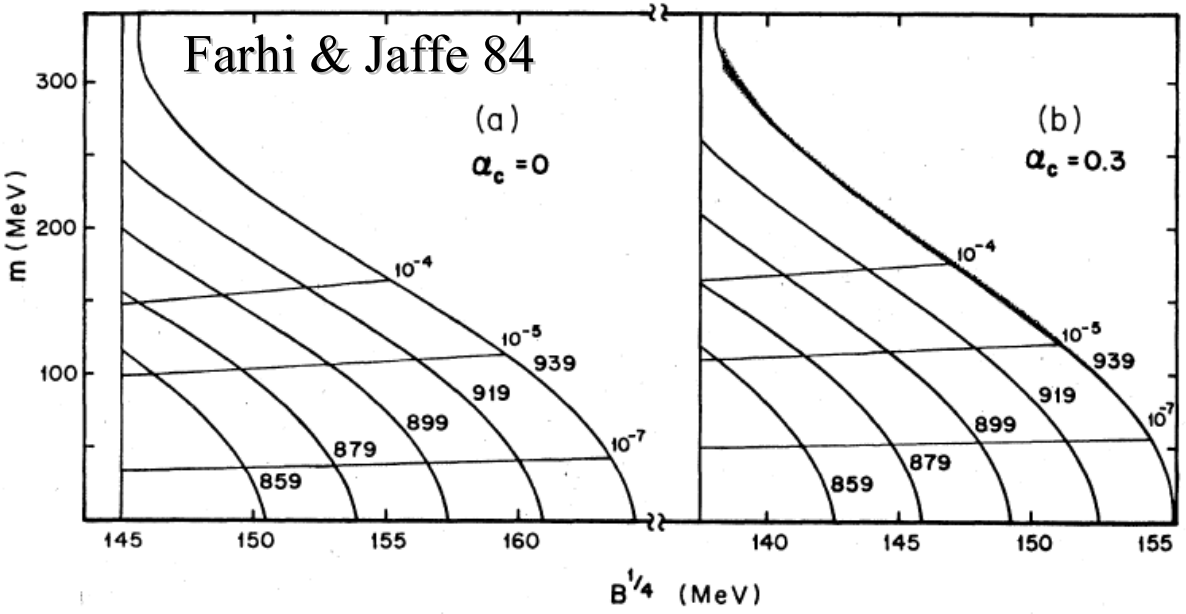

Masses of "strange matter nuclei": even if strange quark matter is stable in the bulk a sufficiently large A (~100) is required to obtain stable strange matter "nuclei" (i.e. strangelets).

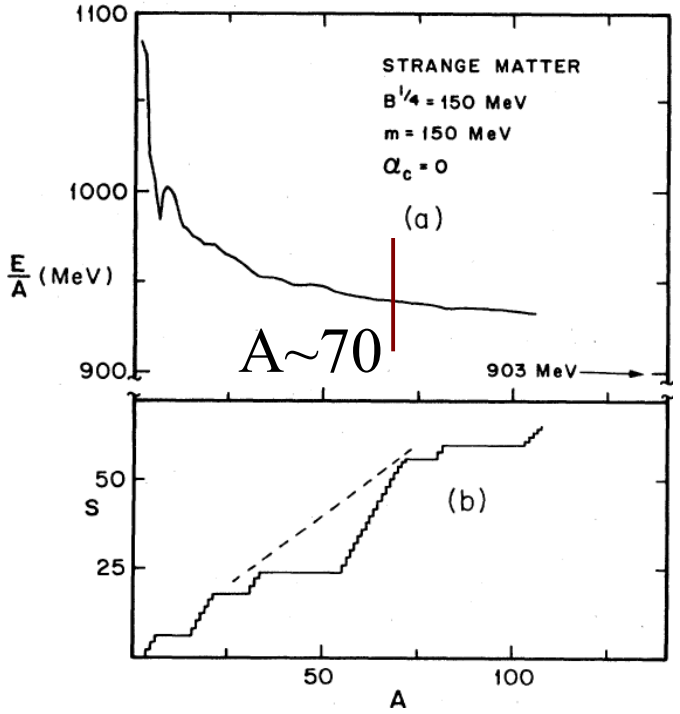

Large values of A:

→ Conversion of ordinary nuclei is very unlikely; need of simultaneous multiple weak interactions.

→ Possible in neutron stars: bulk matter with densities up to 10 n_0. In dense matter strangeness naturally appears at densities of the order of $2n_0$ through hyperons.

Self-bound strange stars *(Haensel et al 86 – Alcock et al 86). Crust: very thin, probably unable to explain glitches and QPOs!!*

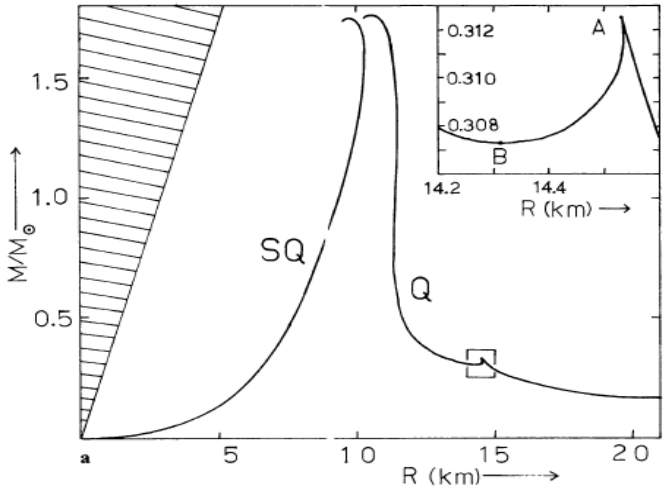

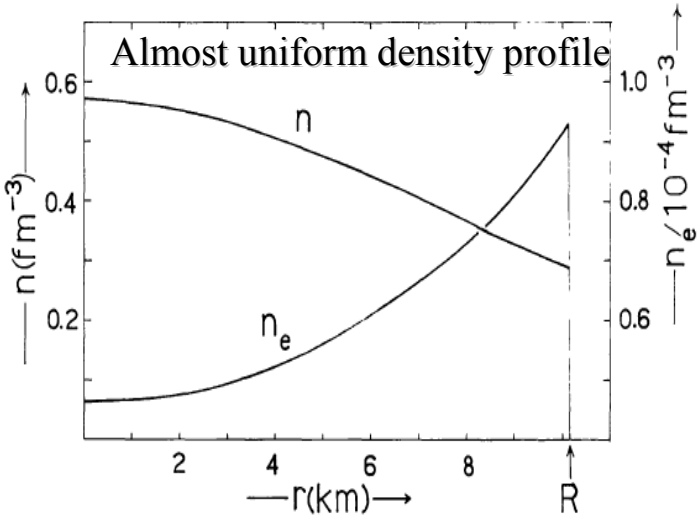

Strangelets in cosmic rays

Two possible sources:

Evaporation of strange matter in the early Universe

Charles Alcock
Center for Theoretical Physics, Center for Space Research and Department of Physics, Massachusetts Institute of Technology, Cambridge, Massachusetts 02139

Edward Farhi
Center for Theoretical Physics, Laboratory for Nuclear Science and Department of Physics, Massachusetts Institute of Technology, Cambridge, Massachusetts 02139
(Received 6 May 1985)

Strange matter, a stable form of quark matter containing a large fraction of strange quarks, may have been copiously produced when the Universe had a temperature of ~100 MeV. We study the evaporation of lumps of strange matter as the Universe cooled to 1 MeV. Only lumps with baryon number larger than $\sim 10^{52}$ could survive. This places a severe restriction on scenarios for strange-matter production.

Strangelets ejected by strange star – strange star mergers

Evidence against a strange ground state for baryons

R.R. Caldwell and John L. Friedman
Department of Physics, University of Wisconsin, Milwaukee, WI 53201, USA

Received 15 October 1990; revised manuscript received 7 May 1991

We argue that if strange quark matter were the ground state of baryons at zero pressure and if some observed compact stars (or some cosmic rays) are strange, then the interstellar medium is so contaminated by strangelets that essentially all "neutron" stars in the disk of the galaxy would have to be quark stars: Strangelet contamination would apparently vastly exceed the minimum abundance needed to seed all newly born neutron stars. Because observed glitches seem not to be compatible with quark stars, a strange quark ground state is unlikely.

Main astrophysical argument againts the strange quark matter hyp.

Strangelets from mergers

1) Event rate of strange stars mergers?
2) Dynamics of the ejecta, ejected mass?
3) Fragmentation, mass spectrum?
4) Capture of strangelets by compact stars (cold and hot), main sequence stars?

Strange star mergers from population synthesis

(Wiktorowicz et al 2017)

StarTrack code by Belczynski 2002

Simulation of 2 millions binaries with three different metallicities, statistical distributions of progenitor masses, binary separation, eccentricities and natal kicks.

Two families scenario: maximum mass of hadronic stars 1.5-1.6 M_{sun} (see in the following). Massive stars are strange stars.

A small modification of the mass distribution around 1.4M_{sun}

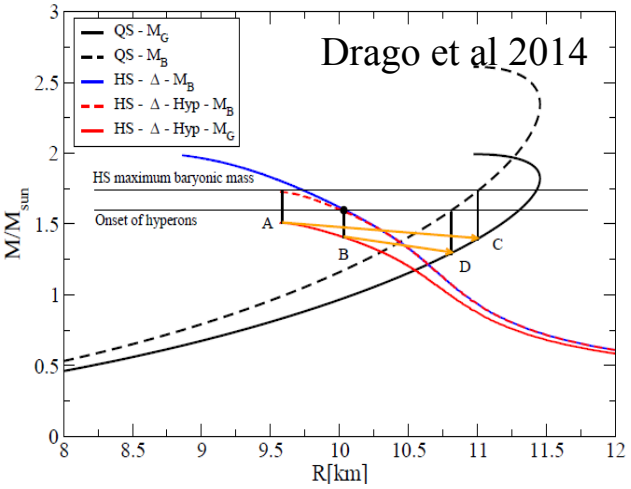

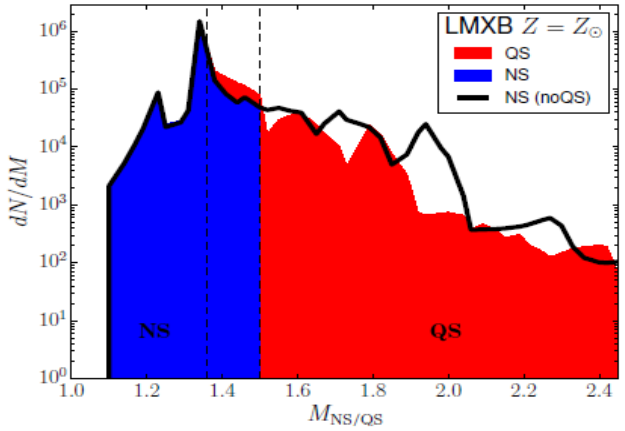

Evolution of two MS stars leading to a double strange star system.

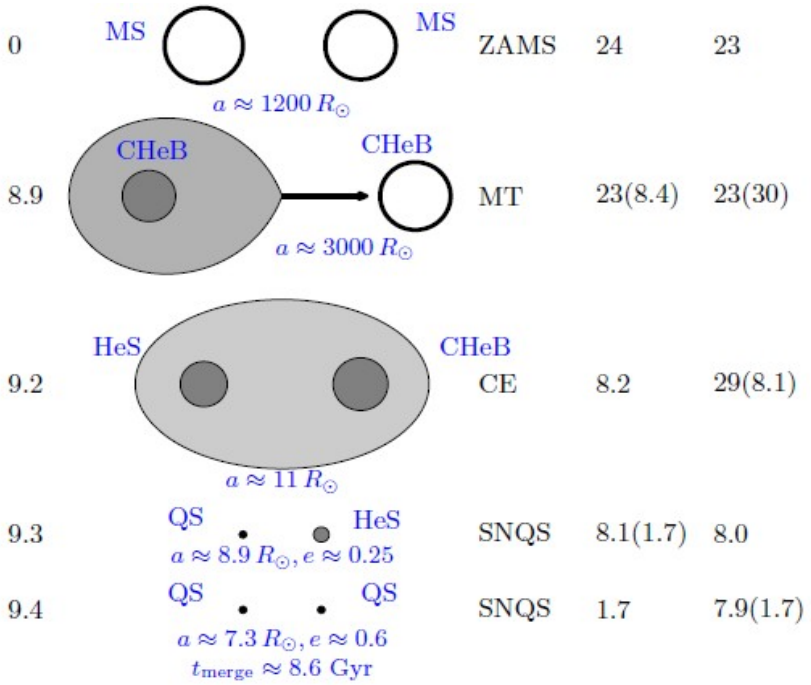

TABLE 1
NUMBER OF QS/NS IN BINARIES

Metallicity	#QS[a]	#NS[a]	$f_{\rm QS}$[b]	#NS(noQS)[c]	$f_{\rm cr}$[d]
		ALL			
$Z_\odot$	9.0×10^4	7.2×10^6	0.01	7.3×10^6	**1.10**
$Z_\odot/10$	2.7×10^5	7.4×10^6	0.04	7.7×10^6	**1.37**
$Z_\odot/100$	1.5×10^5	1.0×10^7	0.01	1.0×10^7	**1.57**
		LMXB			
$Z_\odot$	1.6×10^4	6.1×10^4	0.26	7.7×10^4	**1.61**
$Z_\odot/10$	1.2×10^4	1.5×10^5	0.08	1.6×10^5	**1.22**
$Z_\odot/100$	7.0×10^3	2.1×10^4	0.25	2.9×10^4	**1.31**
		DQS/DNS			
$Z_\odot$	–	6.4×10^5	–	6.6×10^5	**0.88**
$Z_\odot/10$	4.2×10^3	5.2×10^5	0.08	5.2×10^5	**1.22**
$Z_\odot/100$	–	7.6×10^5	–	7.6×10^5	**0.86**

NOTE. — QS and NS quantities per MWEG at present time for $M^H_{\rm max} = 1.5\,M_\odot$. ALL – all binaries; LMXB – mass-transferring binaries; DQS/DNS – double QS/NS.

[a] Number of QS (#QS) and NS (#NS)

[b] fraction of QSs; defined as $f_{\rm QS} := \#{\rm QS}/(\#{\rm QS} + \#{\rm NS})$

[c] number of NSs in the model without QSs (noQS)

[d] change in a number of compact objects (QSs and NSs) in $1.36 - 1.5\,M_\odot$ mass range; $f_{\rm cr} := (\#{\rm QS}' + \#{\rm NS}')/\#{\rm NS}'(noQS)$ (mass range marked with $'$)

Estimated rate of DQS mergers (taking into account the coalescence time): 10/Gyr per MW galaxy

Strange quark matter ejecta

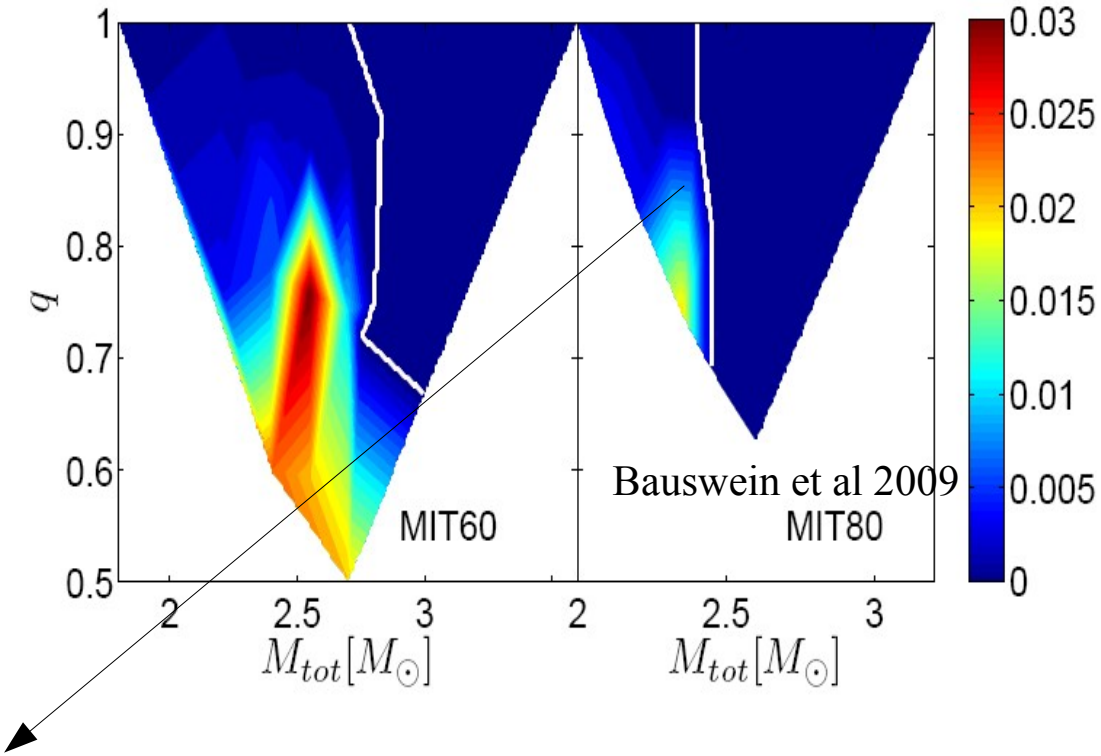

Prompt collapse: in those cases no matter ejected (limited by the numerical resolution $10^{-6}\,M_{sun}$). In the case of matter ejected , average mass $10^{-4}\,M_{sun.}$

To obtain an upper limit: take the typical value of NS mergers, $10^{-2}\,M_{sun}$, use the DQS merger rate: $\rho_s = 10^{-35\,-36}$ g/cm^3.

Flux of strangelets (with a specific value of mass number A, v: velocity of the galactic halo)

$$\frac{\mathrm{d}j_s}{\mathrm{d}\Omega} = \frac{\rho_s v}{4\pi A m_p}$$

$$\mathrm{d}j_s/\mathrm{d}\Omega \sim 10^{-5}\rho_{35}/A \ \mathrm{cm}^{-2}\ \mathrm{s}^{-1}\ \mathrm{sr}^{-1}$$

From Weber 2005

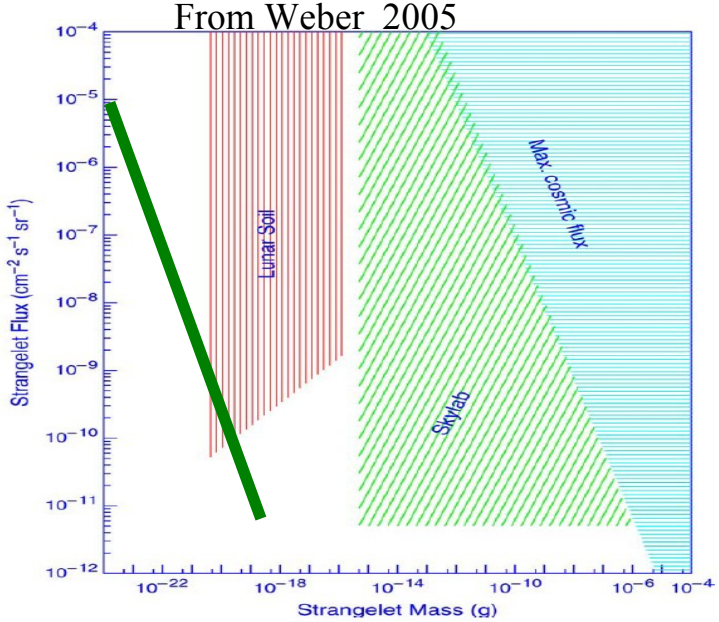

Considering the extreme upper limit on the mass ejected, our fluxes are compatible with the lunar soil searches.

Constraints from PAMELA: our upper limit violates the limits for A<10^3... but the mass ejected is probably much smaller+difficult to fragment down to such small values of A, see in the following PAMELA coll. 2015

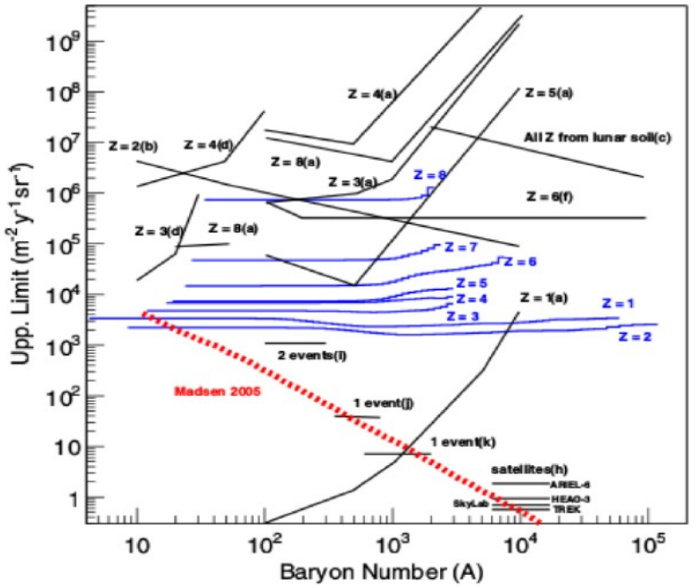

Fragmentation

Work in progress

Condition to create a fragment: Weber number We larger than 1

We=$(\rho/\sigma)\ v^2_{turb}\ d$ (mass density, surface tension, turbulent velocity and drop size). By assuming v^2_{turb} to scale (Kolmogorov) with $v^2_0\ (d/d_0)^{5/3}$ where d_0 ~1km and v_0 ~0.1c , we obtain d ~1mm and thus A ~ 10^{39} very big fragments. There will be a further "reprocessing" via collisions, turbulence, evaporation … very difficult problem!! There will be a distribution of mass number, with a minimum value which is probably much higher than 10^3 .

Depending on the size, different strangelets can act as seeds for the conversion of stars into strange stars (astrophysical argument againts the Witten's hyp.).

Capture of strangelets by stars and conversion

$$mv(x)\frac{dv(x)}{dx} = -\alpha\rho(x)v^2(x) + \frac{GM(x)m}{R^2(x)} - \epsilon(x)\alpha$$

Stopping force due elastic interaction with atoms

Interaction with the ion lattice

Main sequence stars: the most important limit. A strangelet can sit in the center of the star and "wait" for the core collapse SN and the neutronization. This would trigger the conversion of all protoneutron stars into strange stars.

But:

1) due to the 10 MeV temperature of the SN they could evaporate

2) Not clear if fragmentation can work over ten orders of magnitude. Work in progress.

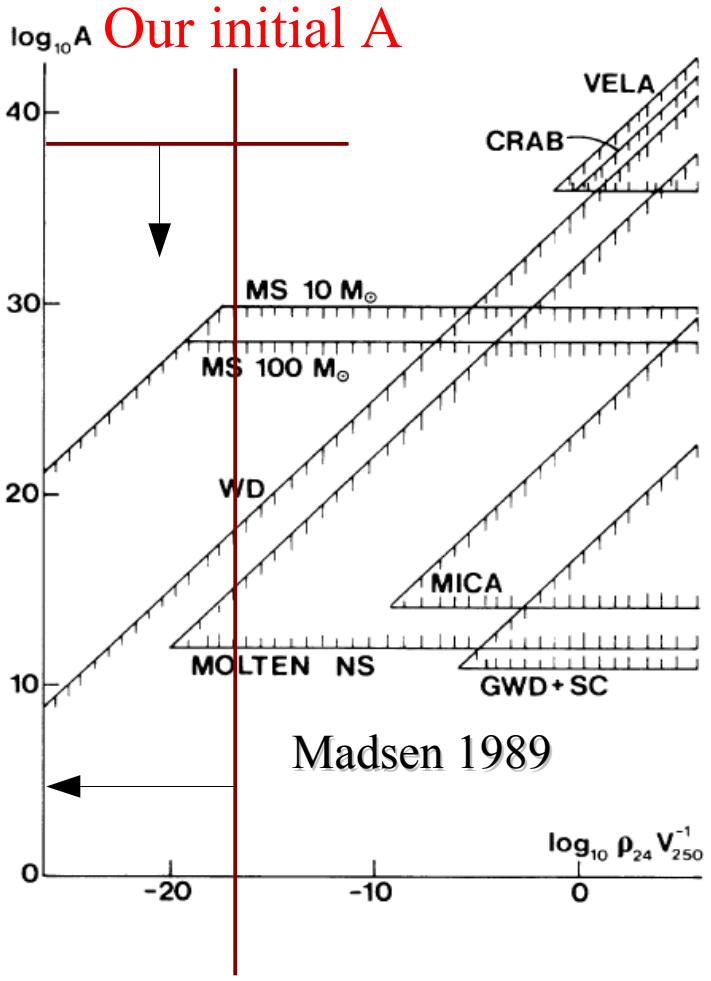

Our upper limit on the strange matter density

A recent intriguing observation
(needs more statistics)

Muon Bundles as a Sign of Strangelets from the Universe

P. Kankiewicz[1], M. Rybczyński[1], Z. Włodarczyk[1], and G. Wilk[2]
[1] Institute of Physics, Jan Kochanowski University, 25-406 Kielce, Poland; pawel.kankiewicz@ujk.edu.pl, maciej.rybczynski@ujk.edu.pl, zbigniew.wlodarczyk@ujk.edu.pl
[2] National Centre for Nuclear Research, Department of Fundamental Research, 00-681 Warsaw, Poland; grzegorz.wilk@ncbj.gov.pl
Received 2016 December 30; revised 2017 March 17; accepted 2017 March 17; published 2017 April 11

Abstract

Recently, the CERN ALICE experiment observed muon bundles of very high multiplicities in its dedicated cosmic ray (CR) run, thereby confirming similar findings from the LEP era at CERN (in the CosmoLEP project). Originally, it was argued that they apparently stem from the primary CRs with a heavy masses. We propose an alternative possibility arguing that muonic bundles of highest multiplicity are produced by strangelets, hypothetical stable lumps of strange quark matter infiltrating our universe. We also address the possibility of additionally deducing their directionality which could be of astrophysical interest. Significant evidence for anisotropy of arrival directions of the observed high-multiplicity muonic bundles is found. Estimated directionality suggests their possible extragalactic provenance.

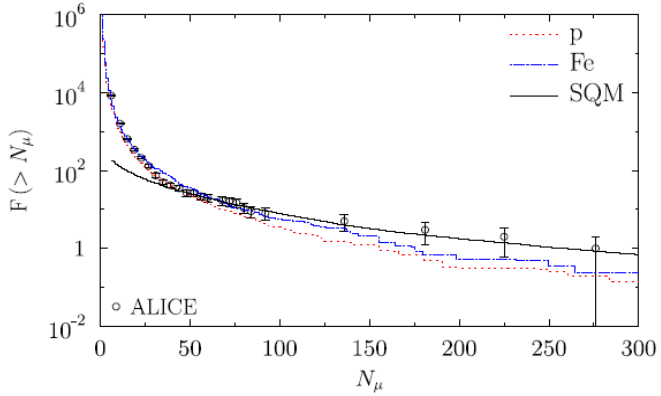

Figure 4. Integral multiplicity distribution of muons for the ALICE data (The ALICE Collaboration 2016b) (circles). Monte Carlo simulations for primary protons (dotted line); iron nuclei (dashed dot line) and primary strangelets with mass A taken from the $A^{-7.5}$ distribution (full line) with abundance (at $A = A_{\rm crit}$) $2 \cdot 10^{-5}$ of the total primary flux.

If true it would imply that also MS stars have captured strangelets

Birth of quark stars
(seeds from hyperons)

1) Nucleation of strange quark matter from hyperonic matter

(not in this talk, see e.g. Iida 98)

2) Expansion and merging of strange quark matter droplets, formation of a strange quark matter core

(not in this talk, see e.g. Horvath et al. 92)

3) Macroscopic conversion of a hadronic star (here!!)

Modeling the conversion

The conversion starts from strange hadronic matter & involves strong interaction (deconfinement) + flavor changing weak interactions u+d->u+s.
Very complicated to model: deconfinement is a non-perturbative phenomenon.

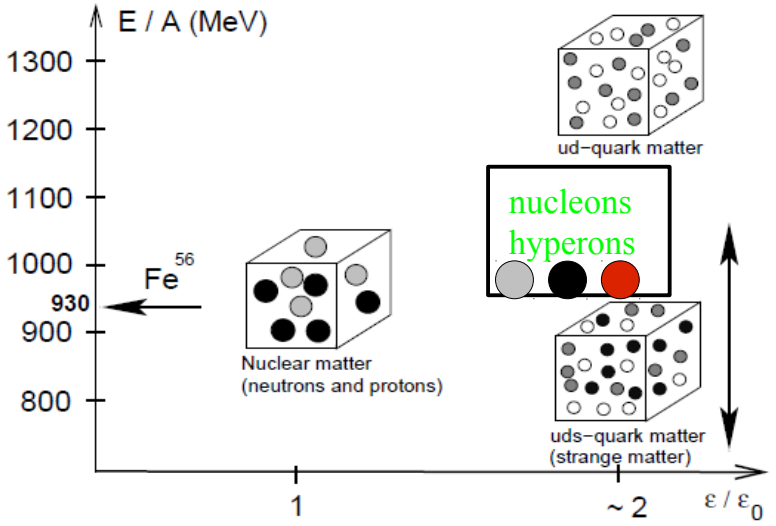

Olinto 87: let us ignore deconfinement and treat the process as a chemical reaction and borrow the formalism of advection-diffusion-reaction PDE

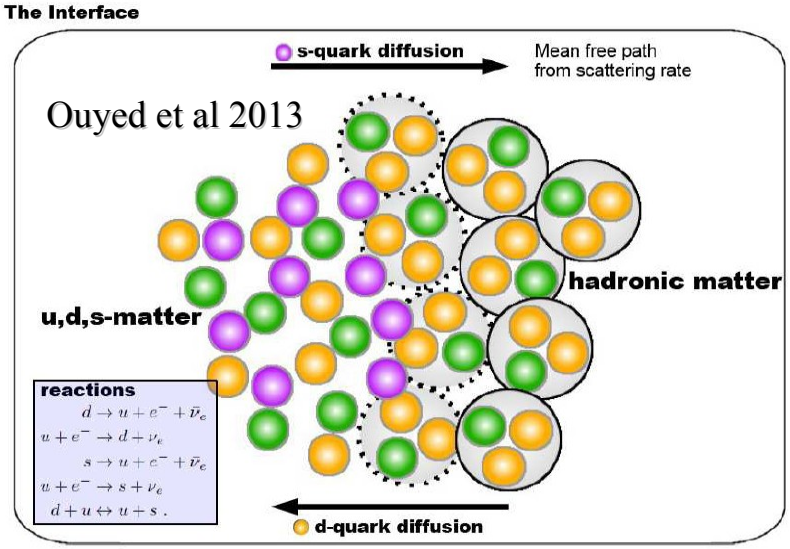

Combustion process

Kinetic theory approach: diffusion of quarks between the two fluids (which are in mechanical equilibrium) and weak interactions

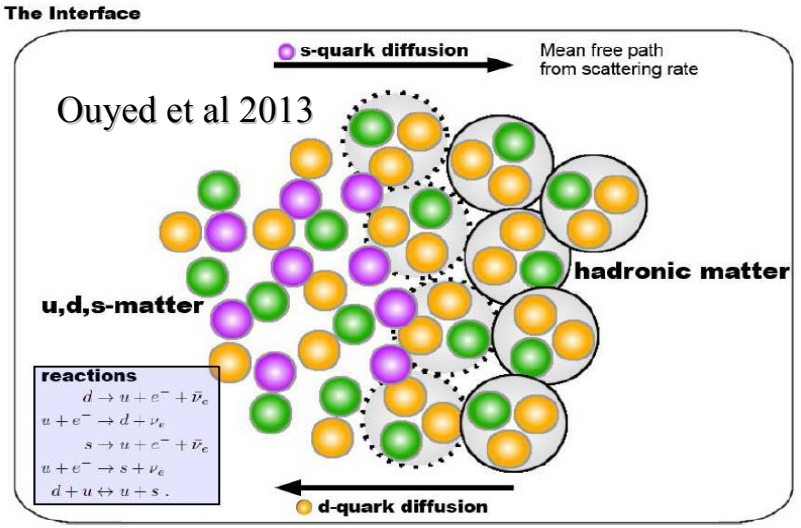

Microphysics: "a" strangeness fraction (n.down-n.strange)/n.baryons

$$D_Q\, a'' - v_{N\to Q}\, a' - \mathcal{R}_Q(a) = 0,$$

$$\mathcal{R}_Q(a) = (\Gamma_{d\to s} - \Gamma_{s\to d})/n_Q,$$

Diffusion coefficient:

$$D \simeq 10^{-1} \left(\frac{\mu_f}{300\ \mathrm{MeV}}\right)^{2/3} \left(\frac{T}{10\ \mathrm{MeV}}\right)^{-5/3} \mathrm{cm}^2/s$$

Typical time scale for u+d->u+s:

$$\tau_Q \simeq 1.3 \times 10^{-9}\,\mathrm{s}\ (300\,\mathrm{MeV}/\mu_Q)^5$$

Dimensional analysis:

1) Typical burning velocity: $v \sim \sqrt{D/\tau} \sim 10^4$ cm/s and scale as $T^{-5/6}$

2)Typical width of the combustion zone: $\delta \sim \sqrt{D\,\tau} \sim 10^{-5}$ cm thus very small in comparison with the size of a star

This approach does not take into account macroscopic flows driven by pressure/density gradients

Coupling with hydrodynamics

Ouyed 2010: 1D – no gravity – no star!

The 1-D hydrodynamical equations in our case are [24]:

$$\frac{\partial U}{\partial t} = -\nabla F(U) + \mathcal{S}(U) \ , \qquad (1)$$

with variables

$$U = \begin{pmatrix} n_s \\ n_s + n_d \\ n_s + n_d + n_u \\ hv \\ s \end{pmatrix} , \qquad (2)$$

and corresponding advective-diffusive terms

$$F(U) = \begin{pmatrix} vn_s + D\nabla n_s \\ v(n_s + n_d) \\ v(n_s + n_d + n_u) \\ hv^2 + P \\ vs \end{pmatrix} , \qquad (3)$$

and source terms

$$\mathcal{S}(U) = \begin{pmatrix} -\Gamma_3 + \Gamma_4 + \Gamma_5 \\ -\Gamma_1 + \Gamma_2 - \Gamma_3 + \Gamma_4 \\ 0 \\ 0 \\ -\frac{1}{T}\sum_i \mu_i \frac{dn_i}{dt} \end{pmatrix} . \qquad (4)$$

Such a calculation would be impossible in 2 or 3D which are needed to study the possible occurrence of hydrodynamical instabilities.

A similar problem when simulating type Ia SN.

Two possible strategies:

1) Khokhlv 1993:

$$\frac{\partial \rho}{\partial t} = -\nabla \cdot (\rho \boldsymbol{U}) \ ,$$

$$\frac{\partial \rho \boldsymbol{U}}{\partial t} = -\nabla \cdot (\rho \boldsymbol{U}\boldsymbol{U}) - \nabla P + \rho \boldsymbol{g} \ ,$$

$$\frac{\partial E}{\partial t} = -\nabla \cdot [(E + P)\boldsymbol{U}] + \rho \boldsymbol{U} \cdot \boldsymbol{g} + \rho \dot{Q} \ ,$$

$$\frac{\partial f}{\partial t} + \boldsymbol{U} \cdot \nabla f = K \nabla^2 f + R$$

K and R are rescaled to enlarge the width of the combustion zone over several computational cells. It underestimates hydro-instabilities.

2) Calculate the burning velocities profiles from the microscopic kinetic theory model, assume an infinitely thin combustion layer.

Hillebrandt 1999 for type Ia SN

Books: Landau, Fluid dynamics.

Ideal-hydro modeling

p: pressure, e: energy density, n: baryon density, w=e+p: enthalpy density, X: $(e+p)/n^2$ dynamical volume, **T**: energy momentum tensor, **u** fluid four velocity, γ: Lorentz factor, j: number of baryons converted per unit of surface and time.

$$T^{\mu\nu} = (e+p)u^\mu u^\nu - pg^{\mu\nu}$$

$$\begin{aligned} \partial_\mu(nu^\mu) &= 0 \\ \partial_\mu T^{\mu\nu} &= 0 \\ e &= e(p,n) \end{aligned}$$

Eqs. of ideal hydrodynamics

Simplifying: let us consider a stationary and 1D physical situation (we consider only the "x" dependence of the fluid variables)

Surface of discontinuity: flame front

e_1 p_1 n_1 | e_2 p_2 n_2

fuel | ashes

Ex: from hydrod. (continuity Eqs.):

$$w_1\gamma_1^2 v_1 = w_2\gamma_2^2 v_2$$

$$p_1 + w_1 v_1^2\gamma_1^2 = p_2 + w_2 v_2^2\gamma_2^2$$

$$n_1 v_1\gamma_1 = n_2 v_2\gamma_2 \equiv j$$

The first two equations can be rewritten as:

$$j^2 = -\frac{(p_2 - p_1)}{(X_2 - X_1)}$$

$$X_2 w_2 - X_1 w_1 = (X_1 + X_2)(p_2 - p_1)$$

This equation defines the so-called *"detonation adiabat"* which is formally identical to a shock adiabat but for the fact that there are two different fluids and thus two different EoS.

Given the initial state 1, and for a fixed value of j (computed from the microphysics model), the state of fluid 2 is determined.

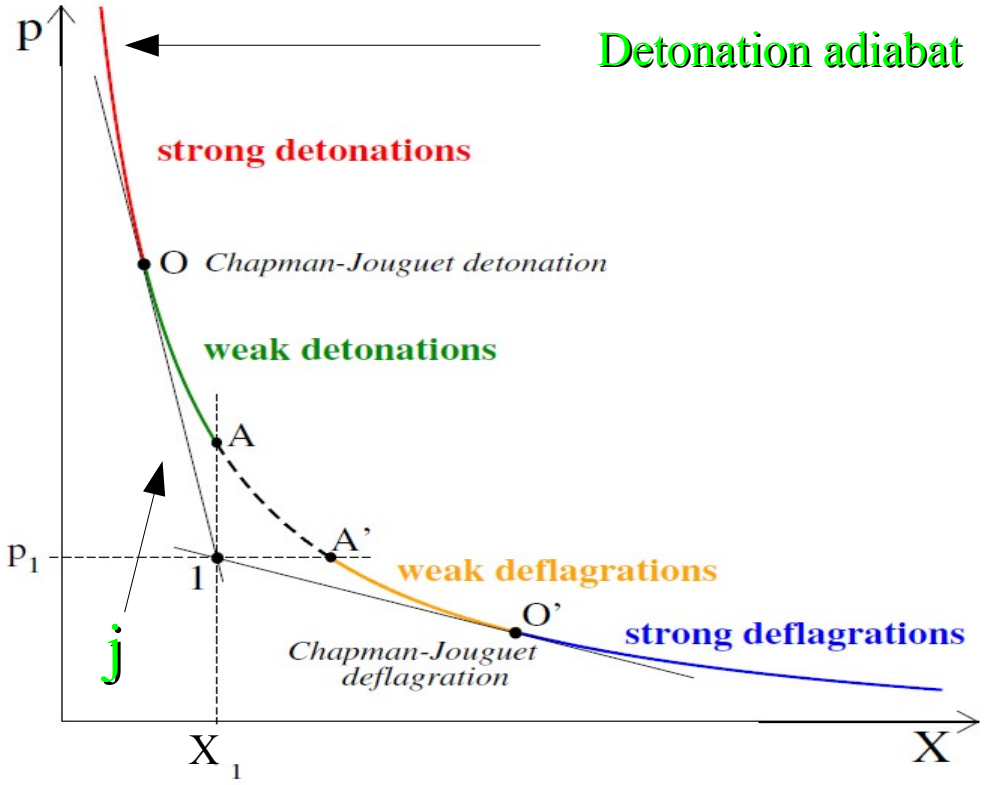

Qualitatively we can distinguish two different combustion modes:
-) *detonation* (the combustion is driven by a shock wave which heats up the fuel thus catalysing the conversion)
-) *deflagration* (the combustion is driven by the microscopic properties: transport of heat/chemical species and rate of reactions)

By introducing the sound velocities in the two fluids c_i

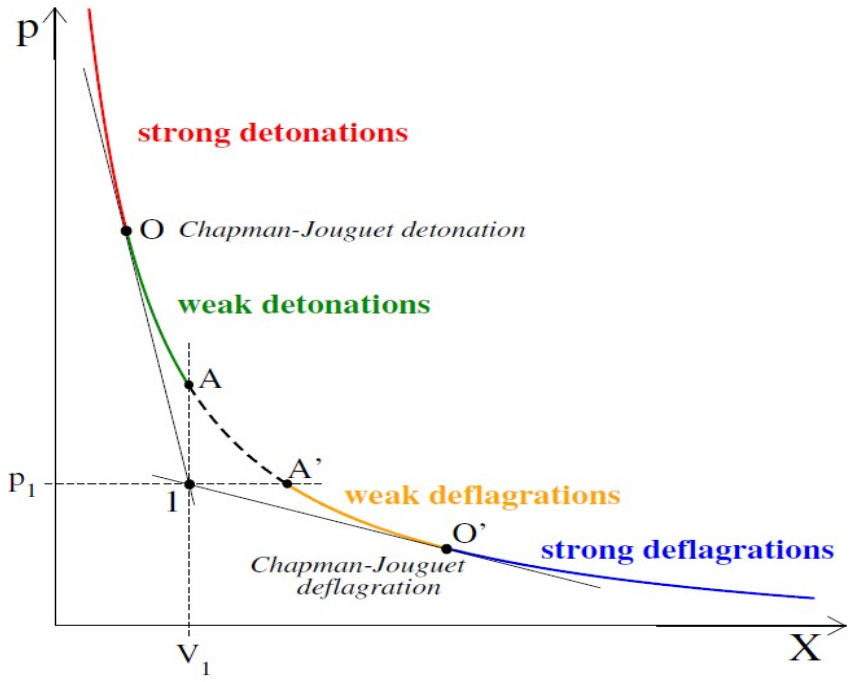

above	O	$v_1 > c_1,\ v_2 < c_2$	strong detonation
on	O	$v_1 > c_1,\ v_2 = c_2$	Chapman – Jouguet detonation
on	AO	$v_1 > c_1,\ v_2 > c_2$	weak detonation
on	AA'	imaginary flux,	no physical significance
on	$A'O'$	$v_1 < c_1,\ v_2 < c_2$	weak deflagration
on	O'	$v_1 < c_1,\ v_2 = c_2$	Chapman – Jouguet deflagration
below	O'	$v_1 < c_1,\ v_2 > c_2$	strong deflagration

Several calculations (see Drago 2007) have shown that in the case of burning of hadronic stars, detonations are quite unlikely. The combustion proceeds as a deflagration.

Numerical simulations of Herzog- Roepke 2011:

-)3+1D code used for SN type Ia simulations
-) Newtonian dynamics + use of an effective relativistic gravitational potential based on TOV (Marek 2006)
-) assume that the combustion proceeds as a deflagration
-) velocity profile taken from Ouyed 2010
-) initial seed: a quark core of 1km which is perturbed with a sinusoidal perturbation of amplitude 0.2 km.
-) EoS: Lattimer-Swesty + MIT bag model
-) 128 or 192 grid cells in each dimension

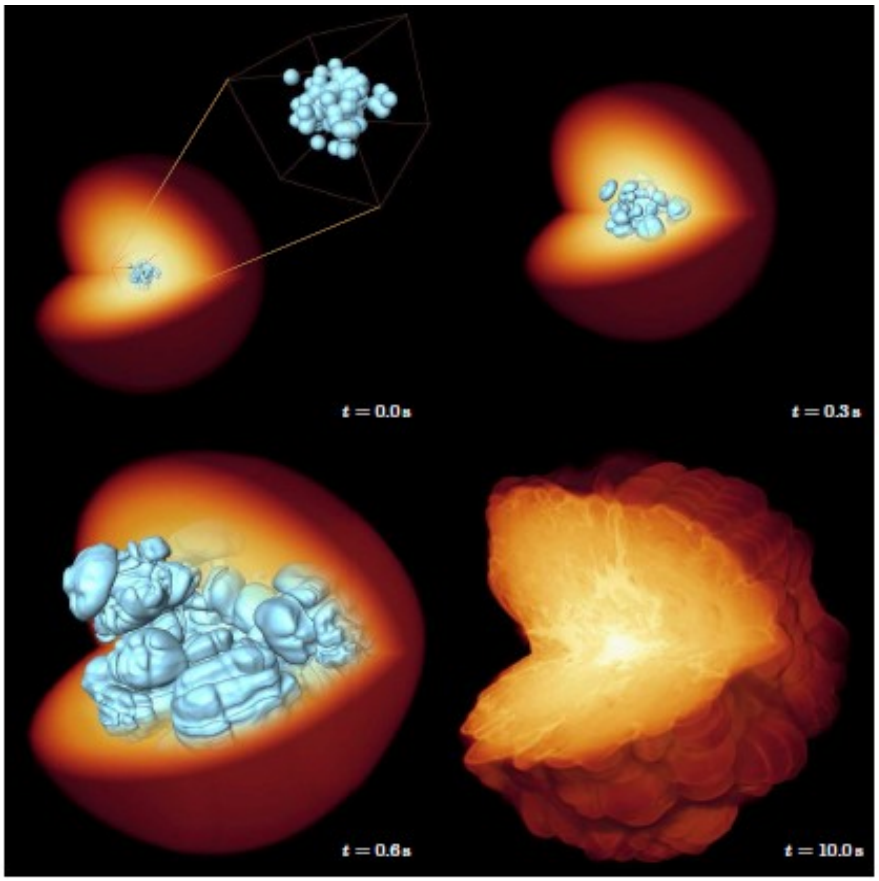

FIGURE 1. Snapshots from a full-star SN Ia simulation starting from a multi-spot ignition scenario. The logarithm of the density is volume rendered indicating the extend of the WD star and the isosurface corresponds to the thermonuclear flame. The last snapshot marks the end of the simulation and is not on scale with the earlier snapshots.

Quark matter seed: 1km + perturbation on the density

Mushroom structures due to hydrodynamical instabilities

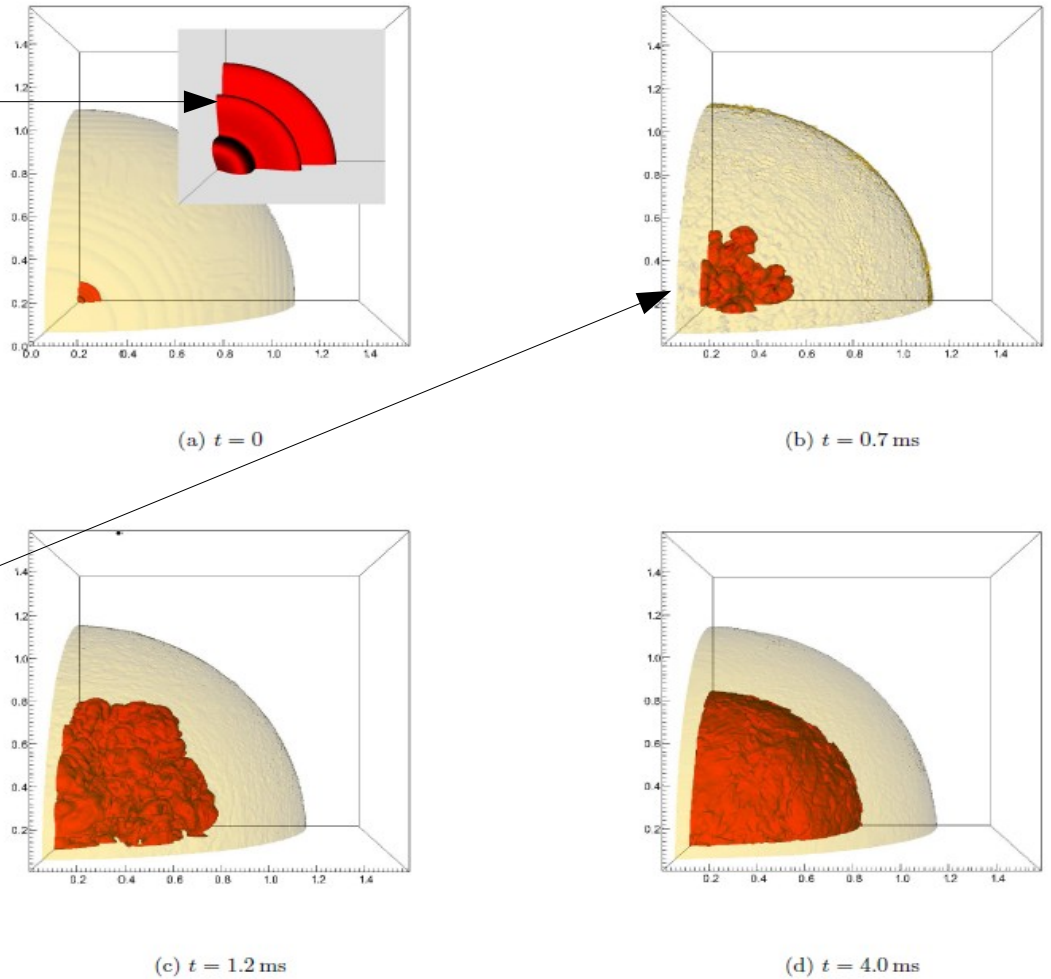

(a) $t = 0$ (b) $t = 0.7\,\mathrm{ms}$

(c) $t = 1.2\,\mathrm{ms}$ (d) $t = 4.0\,\mathrm{ms}$

FIG. 8. (color online) Model B150_192: Conversion front (red) and surface of the neutron star (yellow) at different times t. In (a) a close-up of the central region is added. Spatial units 10^6 cm.

Time needed for the partial conversion: few ms, burning velocities substantially increased by Rayleigh-Taylor instabilities.

-)Effective velocities of conversion increased by several orders of magnitude wtr to the laminar velocities obtained within the purely kinetic theory approach (importance of multiD-hydro)

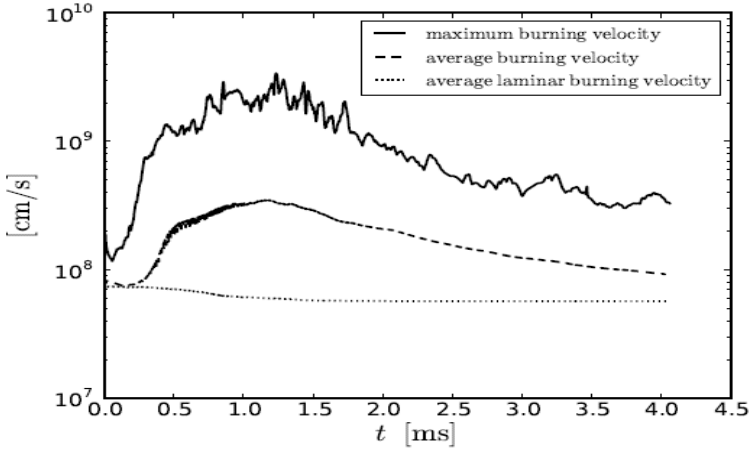

FIG. 7. Burning velocity: Comparison at each timestep of maximum burning velocity, average burning velocity and the underlying average laminar burning velocity. The averages where done over all cells in which burning occurs. Data from the high resolution run with $B^{1/4} = 150\,\mathrm{MeV}$ (model B150_192).

-) Puzzling result: even if the strange quark matter hyp is assumed to hold true, some material (few 0.1 Msun) is left unburnt. The final configuration is similar to a hybrid star. Is this configuration stable?

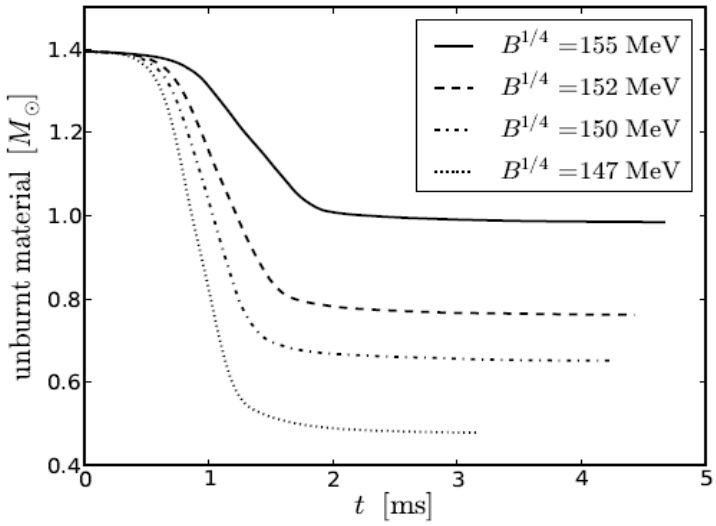

Coll's condition

Coll's condition for “exothermic” combustion (1976), the energy density (or the enthalpy density) of the fuel must be larger than the energy density of the ashes at the same pressure p and dynamical volume X

$$e_1(p, X) > e_2(p, X)$$
$$w_1(p, X) > w_2(p, X)$$

If fulfilled, it implies that the initial point (in the hadronic phase) lies in the region of the p-X plane below the detonation adiabat

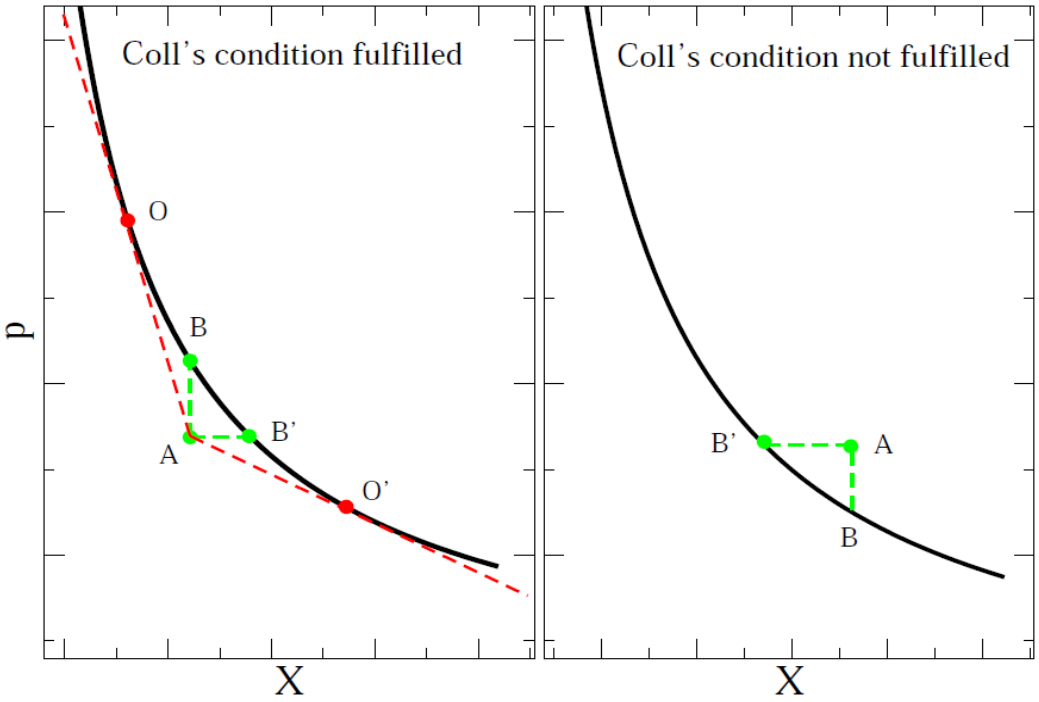

Proof

Let us consider an initial state A in hadronic matter (fixed pressure, energy density, baryon density). We consider for simplicity the EoS of massless quark for quark matter

$$e_q = 3p_q + 4B$$

Let us fix the state B of quark matter (which lies on the detonation adiabat) to have the same dynamical volume of the state A. $(X_A = X_B)$

We want to prove that $p_B > p_A$ provided that the Coll's condition holds true.

Let us define:

$$\Delta(p, X) = e_h(p, X) - e_q(p, X) = w_h(p, X) - w_q(p, X) > 0$$

The detonation adiabat reads:

$$\begin{aligned}
w_h(p_A, X_A) - w_q(p_B, X_A) &= 2p_A - 2p_B \\
e_h(p_A, X_A) + p_A - e_q(p_B, X_A) - p_B + e_q(p_A, X_A) - e_q(p_A, X_A) &= 2p_A - 2p_B \\
\Delta(p_A, X_A) + e_q(p_A, X_A) - e_q(p_B, X_A) &= p_A - p_B \\
\Delta(p_A, X_A) + 3p_A + 4B - 3p_B - 4B &= p_A - p_B \\
\Delta(p_A, X_A) = 2(p_B - p_A)
\end{aligned}$$

Which implies that if Δ>0, then $p_B > p_A$ therefore the initial state A lies in the half-plane below the detonation adiabat.

Ex.: prove it for a polytrope

$$p_q = k n_q^{\gamma}$$
$$e_q = \alpha n_q + p_q/(\gamma - 1)$$

If $e_h(p, X) = e_q(p, X)$ the initial point lies on the detonation adiabat. Moreover, besides the energy density and the pressure, also the baryon density is continuous across the flame front.

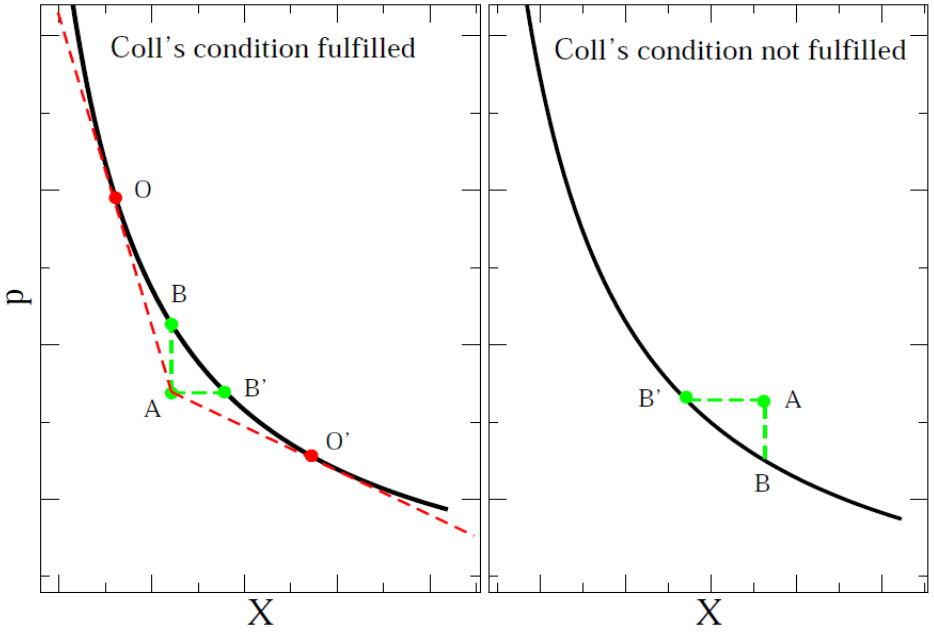

If Coll's condition is not fulfilled, there are no Chapman-Jouguet points. No detonation is possible in the star (detonation with no external forces exists only as a Chapman-Jouguet detonation (Landau)).

What about deflagrations? Let us consider the case of a slow combustion (velocity much smaller than the sound velocity, j ~0 or $p_A \sim p_{B'}$).
In this case the detonation adiabat leads to the conservation of the entalpy per baryon i.e.

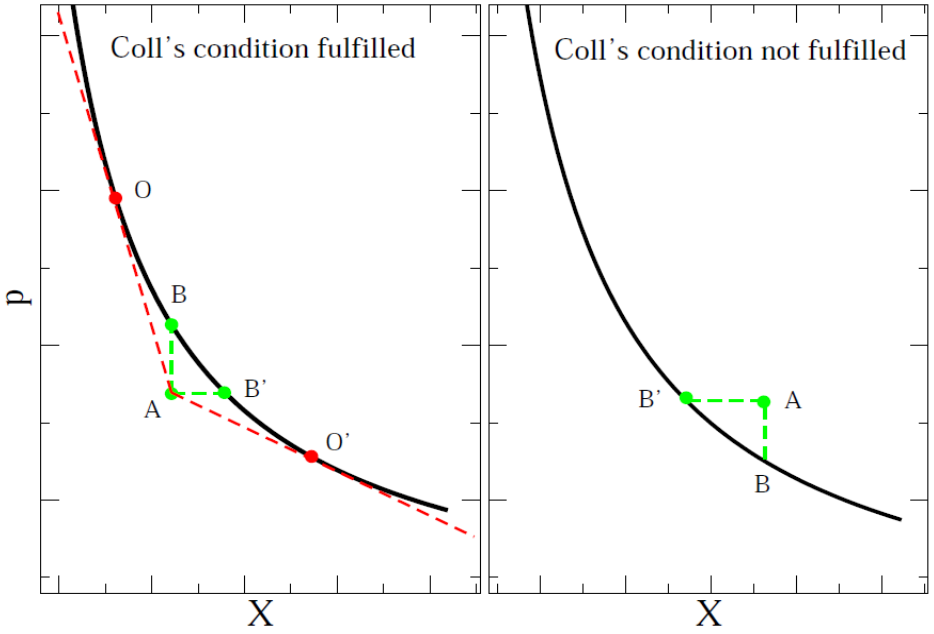

$$(e_A + p_A)/n_A = (e_{B'} + p_A)/n_{B'}$$

Coll's condition implies that

$$X'_B > X_A$$

$$(e_{B'} + p_A)/n_{B'}^2 > (e_A + p_A)/n_A^2$$

$$n_{B'} < n_A$$

$$n_A(e_{B'} + p_A) = n_{B'}(e_A + p_A) < n_A(e_A + p_A)$$

$$e_{B'} < e_A$$

Punch-line: Coll's condition (for the case of a slow combustion) implies that the new phase is produced at a energy density smaller than the one of the fuel: quark matter is lighter than hadronic matter. Inverse density stratification: within the star the gravitational potential and the density gradient point in opposite directions: buoyancy and Rayleigh-Taylor instabilities. If it is violated no instabilities and the velocity of conversion coincides with the (small) laminar velocity (the turbulent eddies stop).

We can define a critical density $\overline{n_h}$ for which $e_h(p, X) = e_q(p, X)$

For different hadronic equations of state it is of ~ 0.2 - 0.3 fm^{-3} (example of massless quarks). Note: hyperons enlarge the window of validity of the Coll's condition.

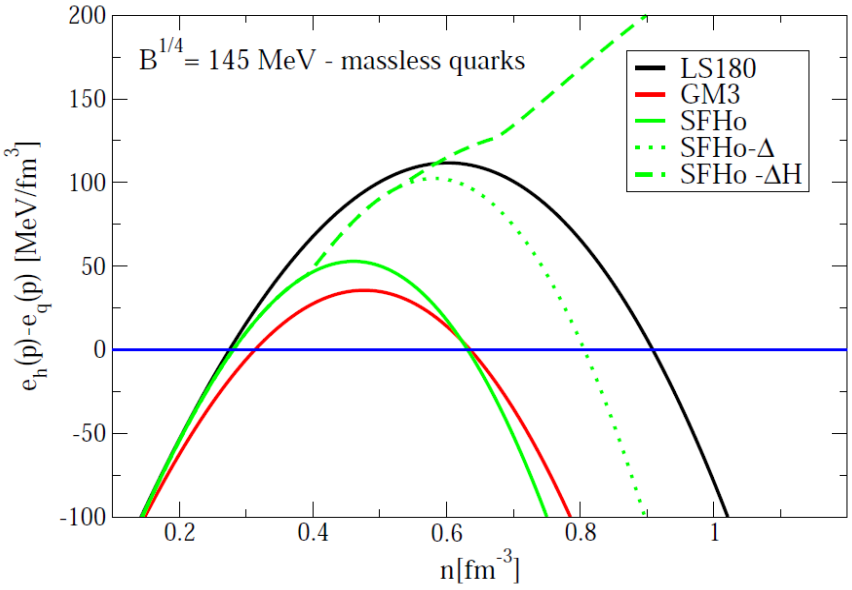

What happens when the combustion front reaches $\overline{n_h}$?

1) At this density, the initial point of the hadronic phase lies on the detonation adiabat:

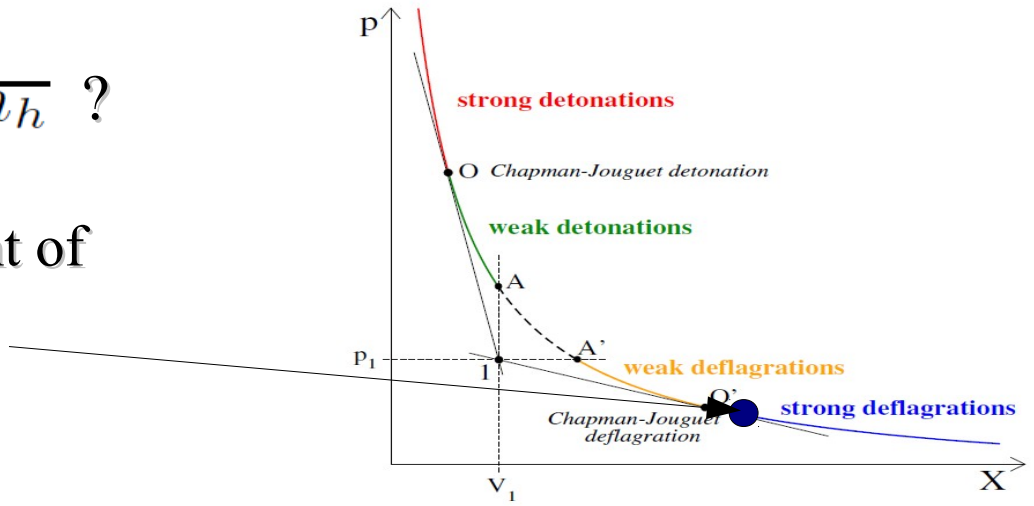

2) End of turbulent eddies and thus of the fast combustion. Beginning of a diffusive regime: time scales much longer than the ones of the turbulent regime.

Fractal model:

$$\gamma = 1 - \frac{e_2}{e_1}.$$

$$v_{mh} = v_{lh}(\lambda_{\max}/\lambda_{\min})^{\Delta D}$$

$$\Delta D = D_0\,\gamma^2$$

Fractal dimension ΔD

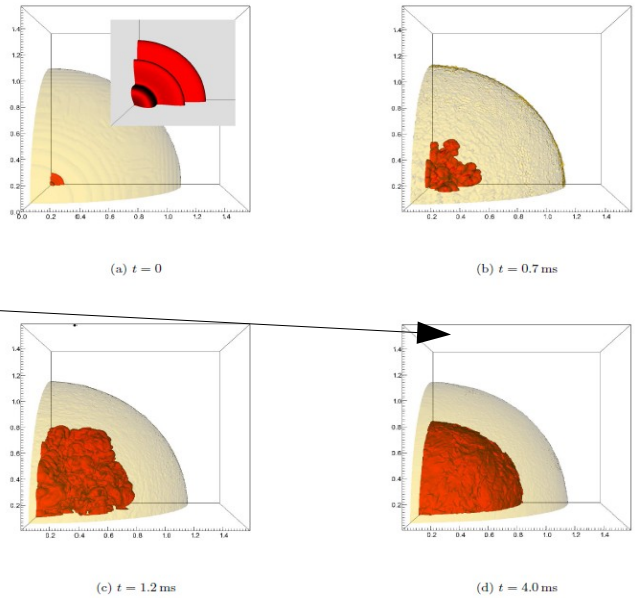

FIG. 8. (color online) Model B150_192: Conversion front (red) and surface of the neutron star (yellow) at different times t. In (a) a close-up of the central region is added. Spatial units 10^6 cm.

The two phases are in mechanical equilibrium. Also energy density and baryon density are continuous across the interface. But: gradient of temperature and of chemical potential. Temperature of the order of few tens MeV in the inner part of the star. Diffusion of heat/chemical species and chemical reactions allow the conversion process to proceed.

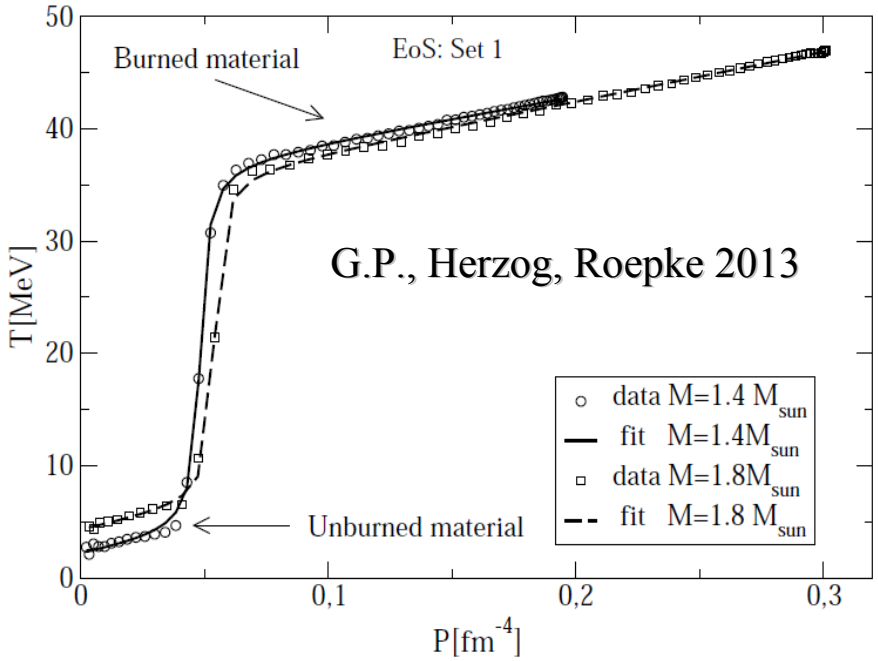

Note: the energy released during the fast conversion (time scales of ms) is emitted by the star on a much longer time scales (order of seconds) through neutrinos. Turbulent conversion and neutrino cooling are decoupled.

Modeling the diffusive regime

During the turbulent conversion both the gravitational mass and the baryonic mass are conserved (no release of neutrinos)

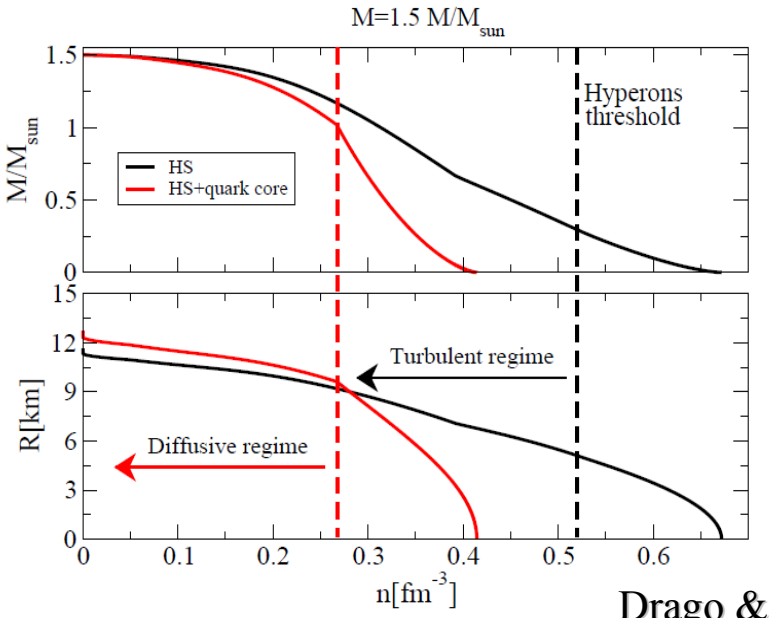

Drago & Pagliara 2015

FIG. 3: Enclosed gravitational mass and radius as a function of the baryon density for a $1.5M_{\odot}$ hadronic star before the turbulent conversion (black lines) and after the turbulent conversion (red lines). The black dashed line marks the appearance of hyperons: the seed of strange quark matter is formed at densities larger than this threshold. The red dashed line marks the density below which Coll's condition is no more fulfilled and the turbulent combustion does not occur anymore. Below this density, the combustion proceeds via the slow diffusive regime.

Profile of a 1.5 Msun hadronic star and a "hybrid star": turbulent conversion can start once hyperons appear, and it will stop 3km below the surface of the star leaving 0.5 Msun which will burn during the diffusive regime.

State of the quark fluid as the conversion proceeds: the two phases are in mechanical equilibrium. The detonation adiabat implies that the enthalpy per baryon is conserved if the cooling process is neglected (Ex: this can be obtained also when applying the first principle of thermodynamics for a transformation at constant pressure and which conserves the total number of baryon).

$$w_A/n_A(p_A, T_A) = w_B/n_B(p_A, T_B)$$

By indicating with N the total number of baryon composing the system, the total enthalpy (for uniform matter) reads:

$$N w_A/n_A(p_A, T_A)$$

After the conversion and once the cooling is complete the system will reach again the same initial temperature (0 in our case). The total enthalpy is therefore: $N w_B/n_B(p_A, T_A)$

One can then define the heat/baryon released by the conversion as:

$$q = w_A/n_A(p_A, T_A) - w_B/n_B(p_A, T_A)$$

Does the conversion proceed until the surface of the star?

At the surface the pressure of the two phases vanishes and the enthalpy/baryon coincides with the energy/baryon.

$$e_A/n_A(T_A = 0, p_A = 0) = e_B/n_B(T_B > 0, p_A = 0) > e_B/n_B(T_B = 0, p_A = 0)$$

Energy/baryon in the crust 930 MeV

Energy/baryon of strange quark matter <930 MeV by hyp.

The conversion is exothermic, and thus spontaneous, until the surface. The hybrid star configurations obtained after the turbulent regime are not stable.

Propagation of the front and cooling

Within the combustion layer: diffusion and flavor changing weak interactions among quarks

$$D = 0.1 \left(\frac{\mu_q}{300\,\mathrm{MeV}}\right)^{2/3} \left(\frac{T}{10\,\mathrm{MeV}}\right)^{-5/3} \mathrm{cm}^2/\mathrm{sec}, \quad \tau = 1.3 \times 10^{-9} \left(\frac{300\,\mathrm{MeV}}{\mu_q}\right)^{5} \mathrm{sec}$$

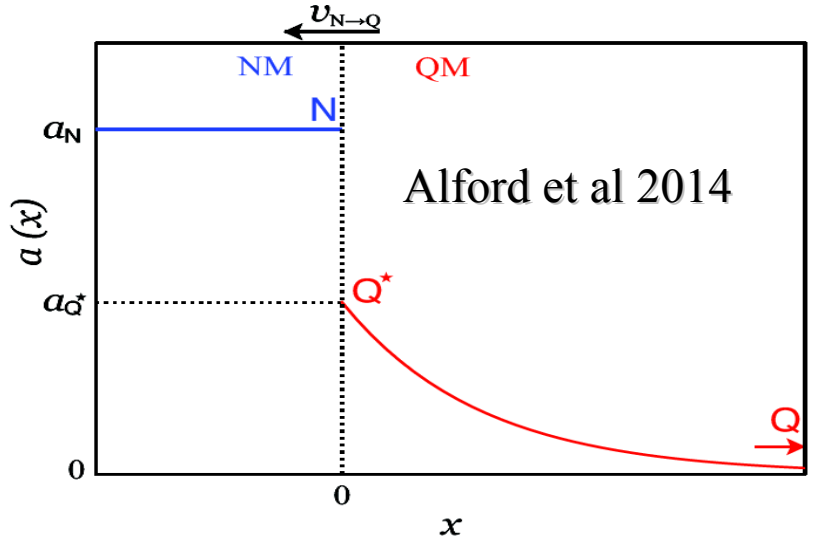

$$v_{lf} = \sqrt{\frac{D}{\tau}\frac{a_{Q*}^4}{2a_N(a_N - a_{Q*})}}$$

At fixed pressure, the minimum amount of strangeness (non-beta stable quark matter) for the process of conversion to be energetically convenient.

-) Uniform temperature, black body emission from the neutrinosphere located at r_s (we have assumed that neutrinos decouple at the inner crust-outer crust interface)

$$\frac{\mathrm{d}r_f}{\mathrm{d}t} = v_{lf}(\mu_q, T)$$

$$C(T)\frac{\mathrm{d}T}{\mathrm{d}t} = -L(T) + 4\pi r_f^2\, j(r_f, T)\, q(r_f, T)$$

$$L = 21/8\sigma(T/K)^4 4\pi r_s^2$$

$$C = 2 \times 10^{39} M/M_\odot (T/10^9)\ \mathrm{erg/K}$$

Source of heat: energy released by the conversion

$v \sim 1/T^{5/6}$ the more material is converted the higher the temperature the slower the velocity. Self-regulating mechanism!

Quasi-plateaux in the neutrino luminosity. Unique feature of the formation of a quark star:

-) no need of a SN (the conversion could occur also for cold neutron stars)

-) if associated with a SN, this emission lasts much longer than the possible extended emission due to the fallback.

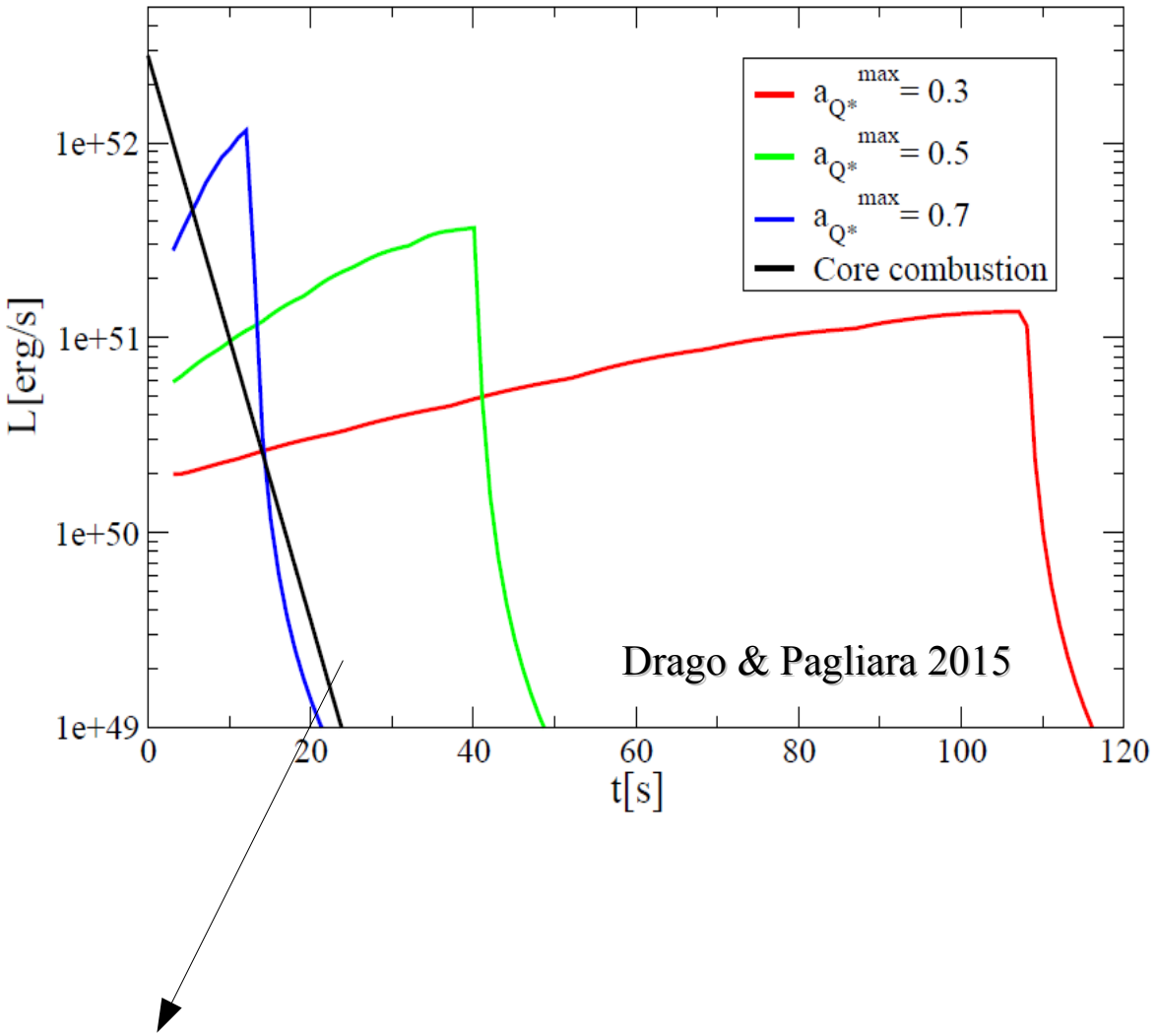

Fast decay of a standard cooling

Strange stars from masses and radii?

What does a $2M_{sun}$ star mean?

"Standard" neutron stars, just nucleons and electrons.

Central baryon densities of a $2M_{sun}$ star 3-7 times nuclear saturation density. Are there really just nucleons? Hyperons & Δ ?

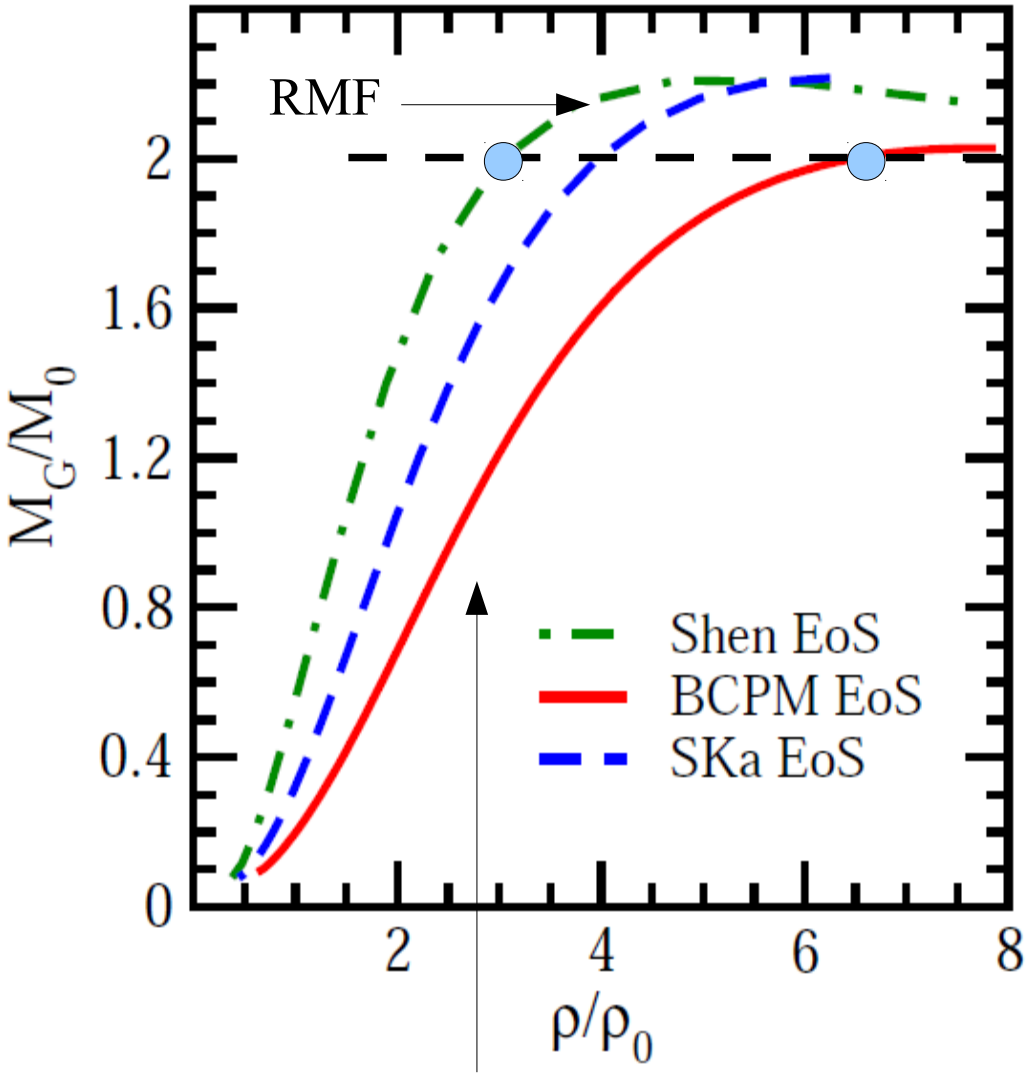

Microscopic calculation: nucleon nucleon potential and three body forces (Baldo et al 2013)

Larger masses from GRBs?

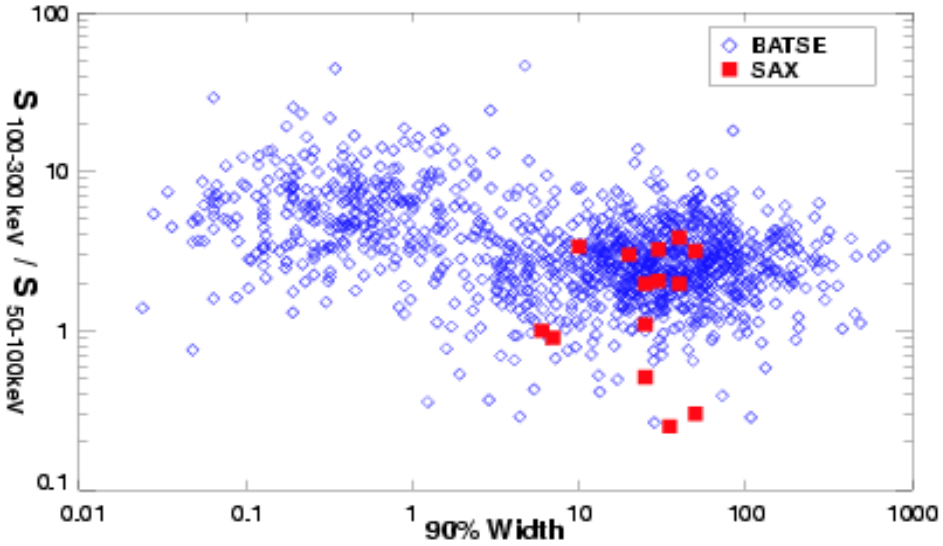

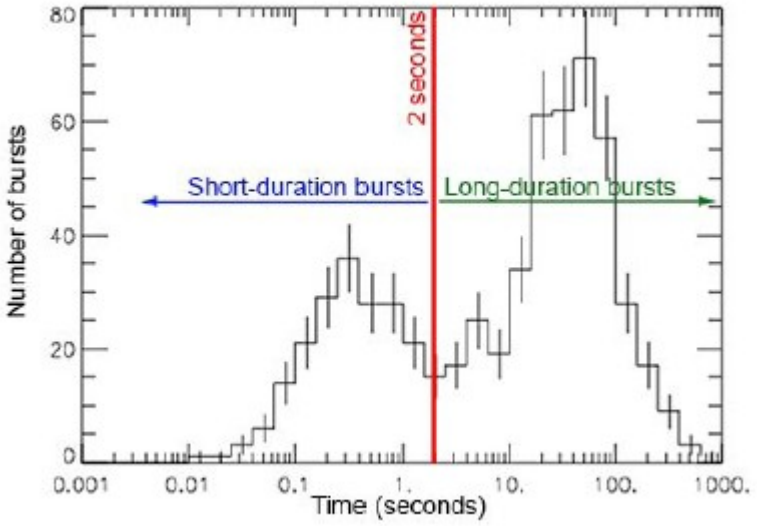

Relativistic jet : $\Gamma \sim 100$

Long: collapse of massive stars – observed connection with Supernovae

Short: not associated with Supernovae- most probably produced by compact stars mergers

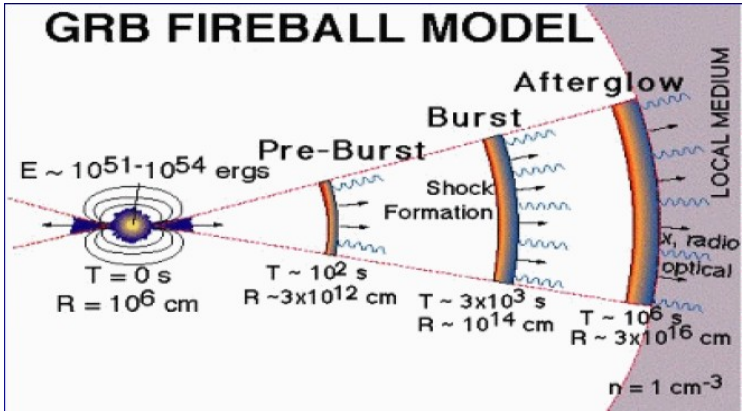

… heavier stars from shortGRB observations?

Before SWIFT: energy released 10^{51} erg, duration few hundreds of ms. Inner engine: merger of two neutron stars with masses of about 1.3-1.5 M_{sun} (main motivation: no SN associated with shortGRB).

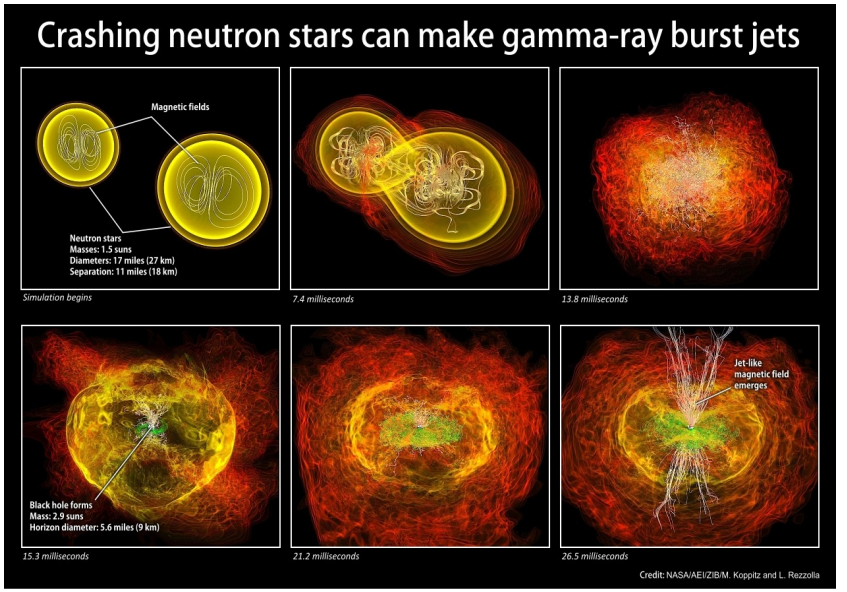

NASA/AEI/ZIB/M. Koppitz and L. Rezzolla

SWIFT has detected many shortGRB with late time activity (10^5sec). This could imply that the remnant of the merger is a compact star and not a black hole!! Maximum mass ~2.4 Msun (but including supramassive stars). How?

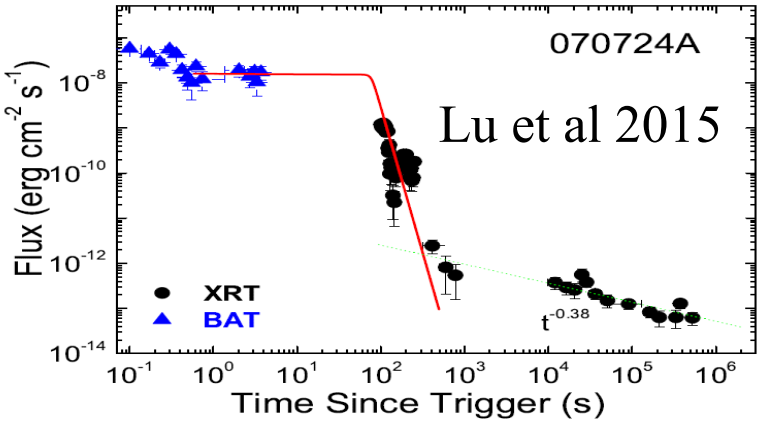

Protomagnetar model: Spin down due to magnetic dipole emision:

$$P(t) = P_0(1 + \frac{4\pi^2}{3c^3}\frac{B_p^2 R^6}{I P_0^2} t)^{1/2}$$

Relation between the maximum mass of a supramassive star and the maximum mass of the non-rotating star (it depends on the EoS)

$$M_{\rm max} = M_{\rm TOV}(1 + \hat{\alpha} P^{\hat{\beta}})$$

Collapse time of the supramassive star (before t_{col} the star emits the signal seen in the plateaux)

$$t_{\rm col} = \frac{3c^3 I}{4\pi^2 B_{\rm p}^2 R^6}[(\frac{M_{\rm p} - M_{\rm TOV}}{\hat{\alpha} M_{\rm TOV}})^{2/\hat{\beta}} - P_0^2]$$

Lu et al 2015

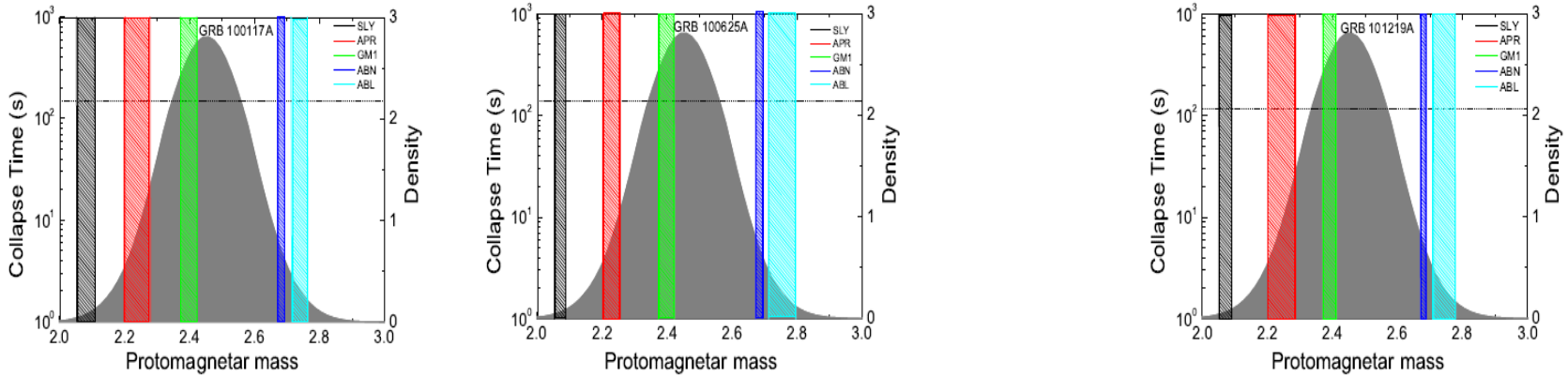

FIG. 11.— Collapse time as a function of the protomagnetar mass. The shaded region is the protomagnetar mass distribution derived from the total mass distribution of the Galactic NS−NS binary systems. The predicted results for 5 equations of state are shown in each panel: SLy (black), APR (red), GM1 (green), AB-N (blue), and AB-L (cyan). The horizontal dotted line is the observed collapse time for each GRB.

Two radii measurements (see talk of Fortin)

THE NEAREST MILLISECOND PULSAR REVISITED WITH *XMM-NEWTON*: IMPROVED MASS–RADIUS CONSTRAINTS FOR PSR J0437–4715

SLAVKO BOGDANOV
Columbia Astrophysics Laboratory, Columbia University, 550 West 120th Street, New York, NY 10027, USA; slavko@astro.columbia.edu
and
Department of Physics, McGill University, 3600 University Street, Montreal, QC H3A 2T8, Canada
Received 2012 July 17; accepted 2012 November 17; published 2012 December 19

ABSTRACT

I present an analysis of the deepest X-ray exposure of a radio millisecond pulsar (MSP) to date, an *X-ray Multi Mirror-Newton* European Photon Imaging Camera spectroscopic and timing observation of the nearest known MSP, PSR J0437–4715. The timing data clearly reveal a secondary broad X-ray pulse offset from the main pulse by ~0.55 in rotational phase. In the context of a model of surface thermal emission from the hot polar caps of the neutron star, this can be plausibly explained by a magnetic dipole field that is significantly displaced from the stellar center. Such an offset, if commonplace in MSPs, has important implications for studies of the pulsar population, high energy pulsed emission, and the pulsar contribution to cosmic-ray positrons. The continuum emission shows evidence for at least three thermal components, with the hottest radiation most likely originating from the hot magnetic polar caps and the cooler emission from the bulk of the surface. I present pulse phase-resolved X-ray spectroscopy of PSR J0437–4715, which for the first time properly accounts for the system geometry of a radio pulsar. Such an approach is essential for unbiased measurements of the temperatures and emission areas of polar cap radiation from pulsars. Detailed modeling of the thermal pulses, including relativistic and atmospheric effects, provides a constraint on the redshift-corrected neutron star radius of $R > 11.1$ km (at 3σ conf.) for the current radio timing mass measurement of 1.76 $M_\odot$. This limit favors "stiff" equations of state.

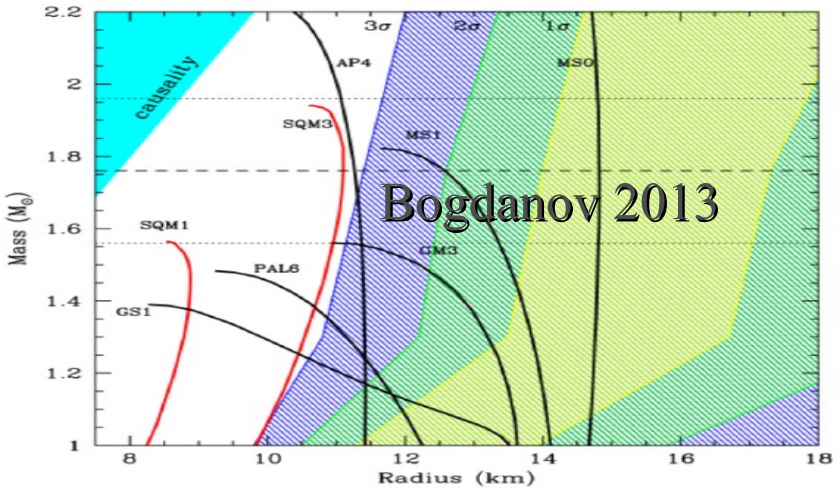

Figure 6. Mass–radius plane for neutron stars showing the 1σ, 2σ, and 3σ confidence contours (yellow, green, and blue hatched regions, respectively) for PSR J0437–4715. The solid lines are representative theoretical model tracks (from Lattimer & Prakash 2001). The horizontal lines show the pulsar mass measurement from radio timing (dashed line) and the associated 1σ uncertainties (dotted lines) from Verbiest et al. (2008).

Different stellar objects, different techniques... still, some indication of large stars (>12 km)
and small stars (<11km)

NEUTRON STAR MASS–RADIUS CONSTRAINTS OF THE QUIESCENT LOW-MASS X-RAY BINARIES X7 AND X5 IN THE GLOBULAR CLUSTER 47 TUC

SLAVKO BOGDANOV[1], CRAIG O. HEINKE[2], FERYAL ÖZEL[3], AND TOLGA GÜVER[4]
[1] Columbia Astrophysics Laboratory, Columbia University, 550 West 120th Street, New York, NY 10027, USA
[2] Department of Physics, University of Alberta, CCIS 4-183, Edmonton AB T6G 2E1, Canada
[3] Department of Astronomy, University of Arizona, 933 North Cherry Avenue, Tucson, AZ 85721, USA
[4] Istanbul University, Science Faculty, Department of Astronomy and Space Sciences, Beyazit, 34119, Istanbul, Turkey
Received 2016 March 4; revised 2016 August 9; accepted 2016 August 18; published 2016 November 7

ABSTRACT

We present *Chandra*/ACIS-S subarray observations of the quiescent neutron star (NS) low-mass X-ray binaries X7 and X5 in the globular cluster 47 Tuc. The large reduction in photon pile-up compared to previous deep exposures enables a substantial improvement in the spectroscopic determination of the NS radius and mass of these NSs. Modeling the thermal emission from the NS surface with a non-magnetized hydrogen atmosphere and accounting for numerous sources of uncertainties, we obtain for the NS in X7 a radius of $R = 11.1^{+0.8}_{-0.7}$ km for an assumed stellar mass of $M = 1.4\ M_\odot$ (68% confidence level). We argue, based on astrophysical grounds, that the presence of a He atmosphere is unlikely for this source. Due to the excision of data affected by eclipses and variable absorption, the quiescent low-mass X-ray binary X5 provides less stringent constraints, leading to a radius of $R = 9.6^{+0.9}_{-1.1}$ km, assuming a hydrogen atmosphere and a mass of $M = 1.4\ M_\odot$. When combined with all existing spectroscopic radius measurements from other quiescent low-mass X-ray binaries and Type I X-ray bursts, these measurements strongly favor radii in the 9.9–11.2 km range for a ~1.5 $M_\odot$ NS and point to a dense matter equation of state that is somewhat softer than the nucleonic ones that are consistent with laboratory experiments at low densities.

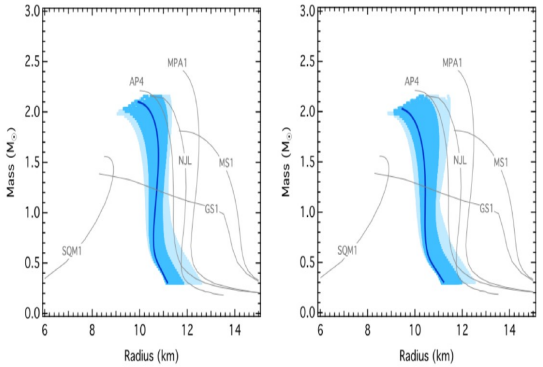

Figure 10. Mass–radius relation (solid blue curve) corresponding to the most likely triplet of pressures that agrees with the current neutron star data. These include the X5 and X7 radius measurements shown in this work, as well the neutron star radii measurements for the 12 neutron stars included in Özel et al. (2016), the low-energy nucleon–nucleon scattering data, and the requirement that the EoS allow for a $M > 1.97\ M_\odot$ neutron star. The ranges of mass–radius relations corresponding to the regions of the $\vec{P}_1, \vec{P}_2, \vec{P}_3$ parameter space in which the likelihood is within $e^{-1/2}$ and e^{-1} of its highest value are shown in dark and light blue bands, respectively. The results for both flat priors in P_1, P_2, and P_3 (top panel) and for flat priors the logarithms of these pressures (bottom panel) are shown.

Bogdanov et al 2016

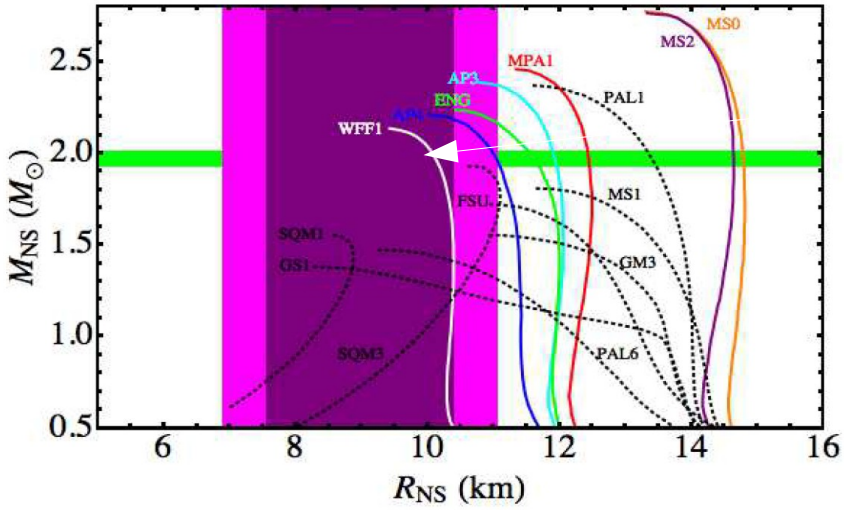

R=9.1±1.3 km. Updated to 9.4±1.2 (September 2014). Debated by Lattimer and Steiner ApJ 2014!!

Wiringa et al 1988, nice, but:

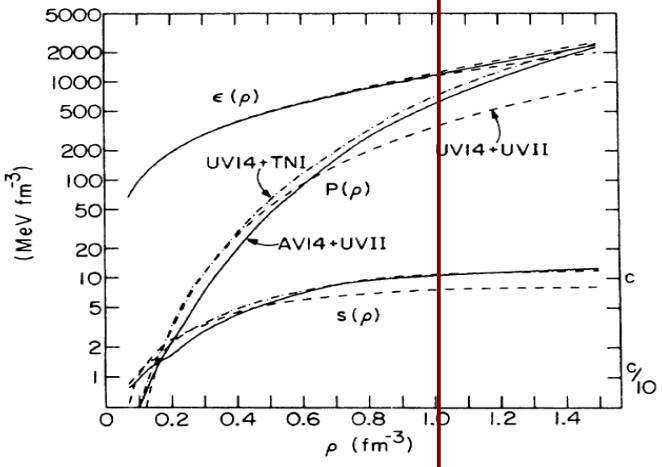

It violates causality

the canonical 1.4 $M_\odot$ neutron star has a central density $\rho_c = 0.57$ fm^{-3} for UV14 plus UVII and 0.66 fm^{-3} for both AV14 plus UVII and UV14 plus TNI, where the

Only nucleons up to very large densities. Similarly for AP4

Tension between different measurements:

high masses → stiff equation of state
small radii → soft equation of state
→ large central densities
→ formation of new particles

Hyperons, deltas?

(see lecture of Lenske and Voskresensky)

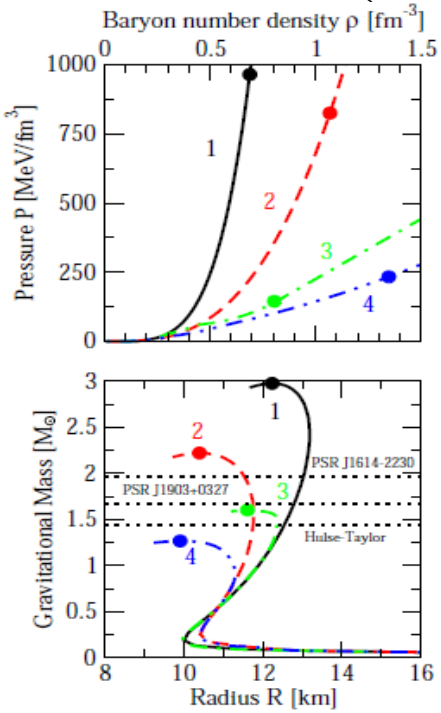

Vidana et al 2011

Lonardoni 2015

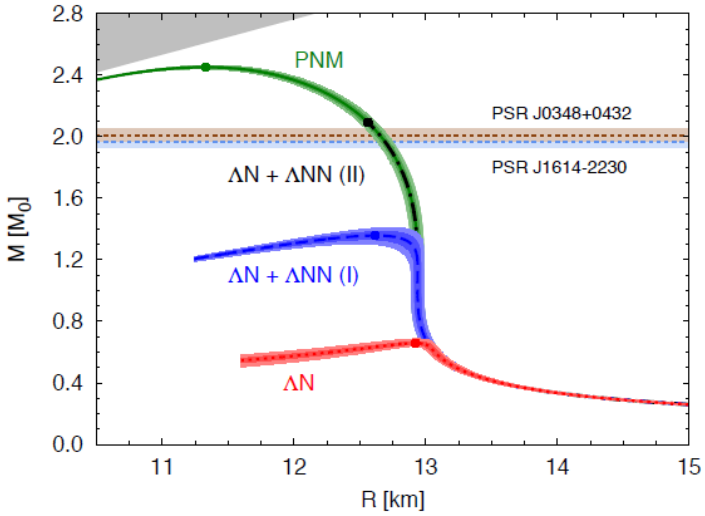

Deltas included

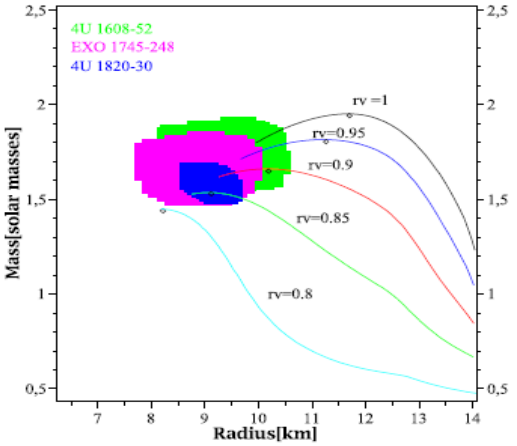

Schurhoff et al 2010

Many possibilities: heavy baryons at very large densities (beyond the density of the maximum mass configuration) or they form in compact stars but the EOS is still stiff enough to fulfill the $2M_{sun}$ limit

Hadronic stars (including hyperons and delta) could be massive (but large) or could be small and light. Only new precise measurements can clarify this problem (hopefully NICER)

Hybrid stars:

Twins stars

(Benic et al 2015, see talk of Blaschke and Alvarez-Castillo)

-) Quark matter appears only in very massive stars.
-) Hybrid stars more compact than hadronic stars
-) 1.4 M_{sun} hadronic stars are large, R >14km

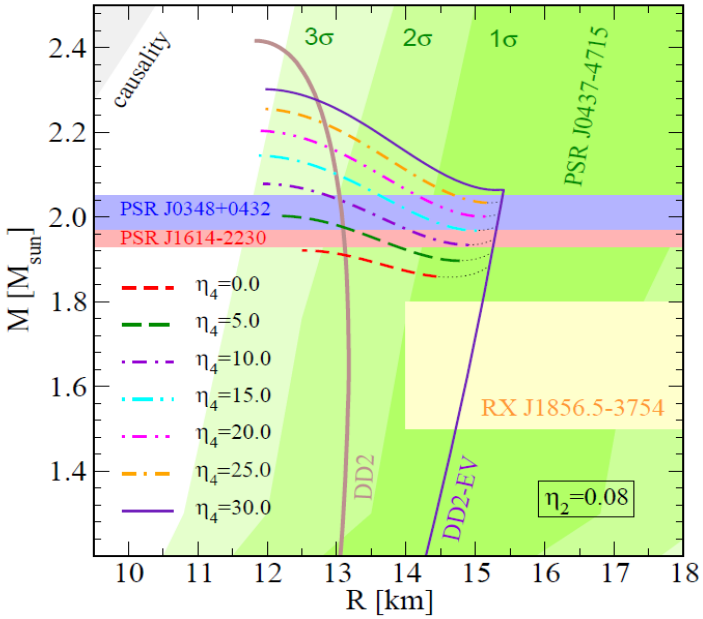

Polytropic parametrizations

(Kurkela et al 2014)

-) mass constraint and pQCD high density constraint:
Radius of the 1.4M_{sun} >11km

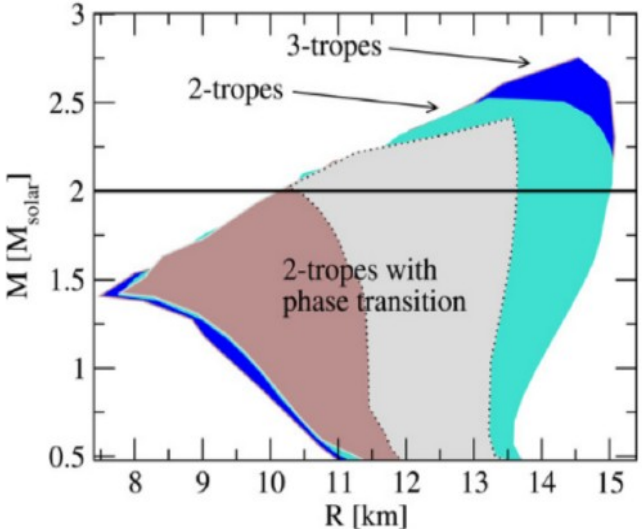

Stars containing quark matter?

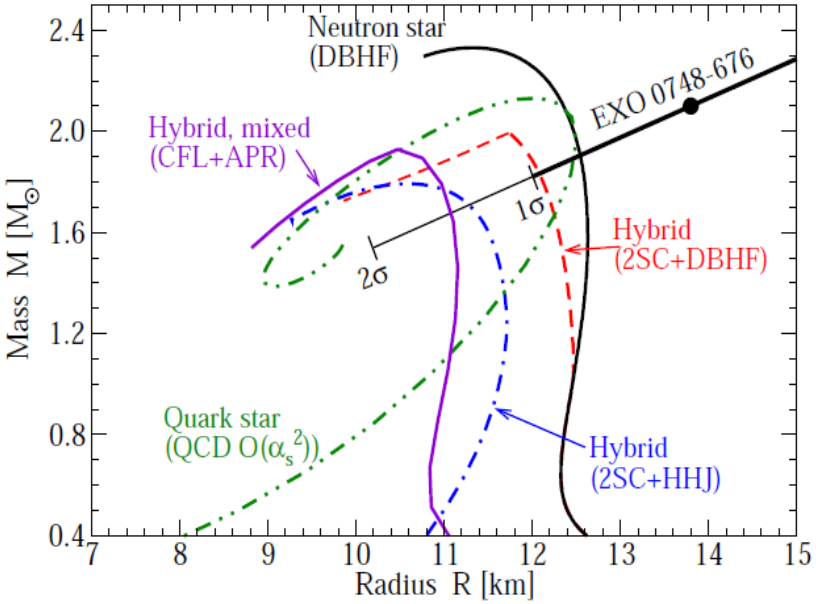

Alford et al Nature 2006

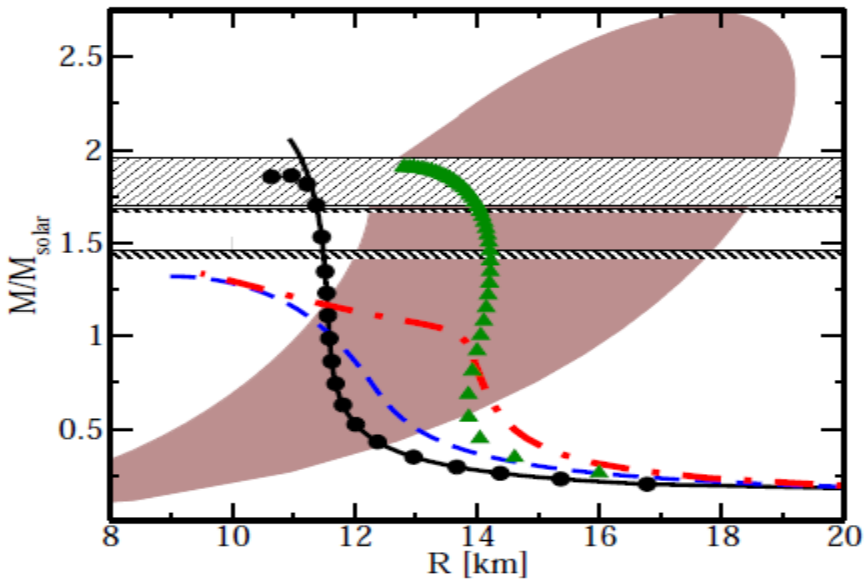

Kurkela et al 2010

pQCD calculations: " ... equations of state including quark matter lead to hybrid star masses up to 2Ms, in agreement with current observations. For strange stars, we find maximal masses of 2.75Ms and conclude that confirmed observations of compact stars with M > 2Ms would strongly favor the existence of stable strange quark matter"

Before the discoveries of the two $2M_{sun}$ stars!!

Two families of compact stars

(exercise with constant speed of sound quark EoS, Dondi et al 2016)

Three parameters:
Speed of sound, energy density and baryon density at pressure=0

$$p = c_s^2(e - e_0)$$

$$k = \frac{e_0 c_s^2}{1+c_s^2}$$

$$p = k((n/n_0)^{1+c_s^2} - 1)$$

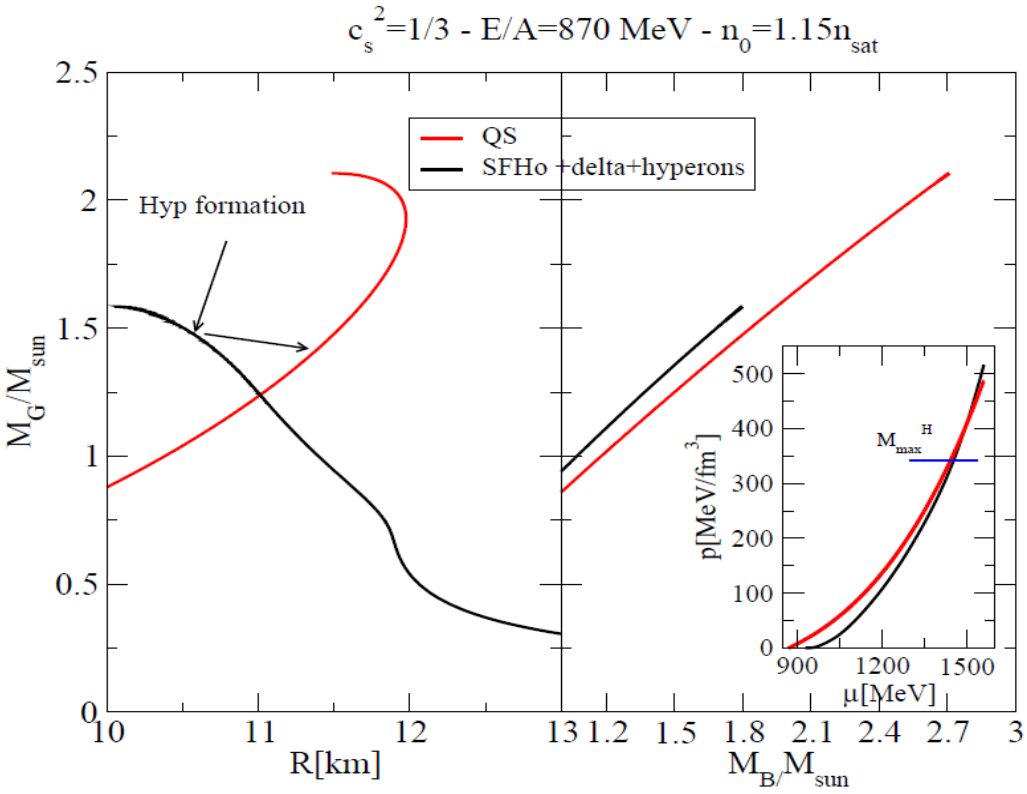

Hadronic stars would fulfill the small radii limits while strange stars would fulfill the large masses limits. Note: at fixed baryon mass, strange stars are energetically convenient even if the radius is larger than the corresponding hadronic star configuration.

Strange quark matter in chiral models

Results of the SU(3) quark meson model as compared with the chiral dielectric model.

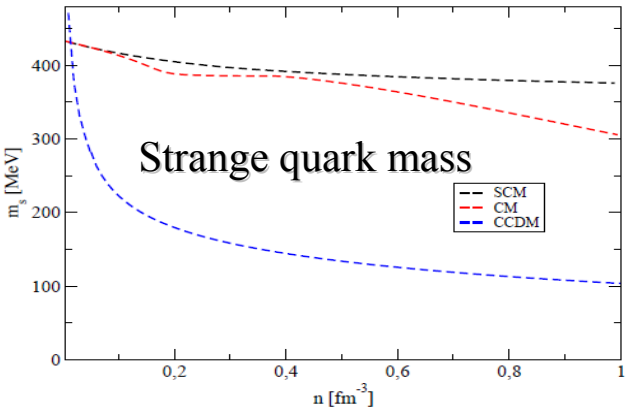

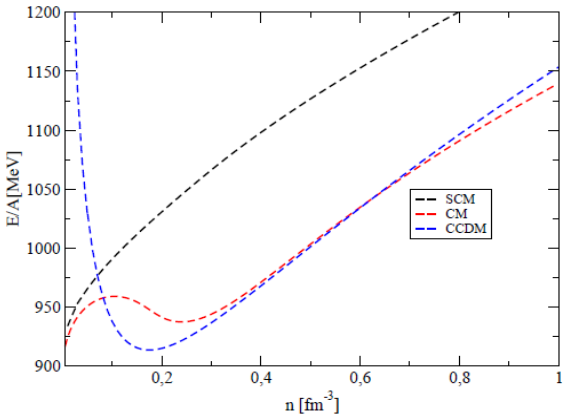

$$\mathcal{L}_\chi = \frac{1}{2}(\partial_\mu \chi)^2 - \frac{1}{2} M_\chi^2 \chi^2 \qquad \mathcal{L}_{int} = -\frac{\sqrt{2}\, g_\sigma}{\chi}(\bar{q} S q)$$

Confinement is realised by making the quark masses divergent at zero density
(similar feauture in the density functional quark model, talk of D. Blaschke)

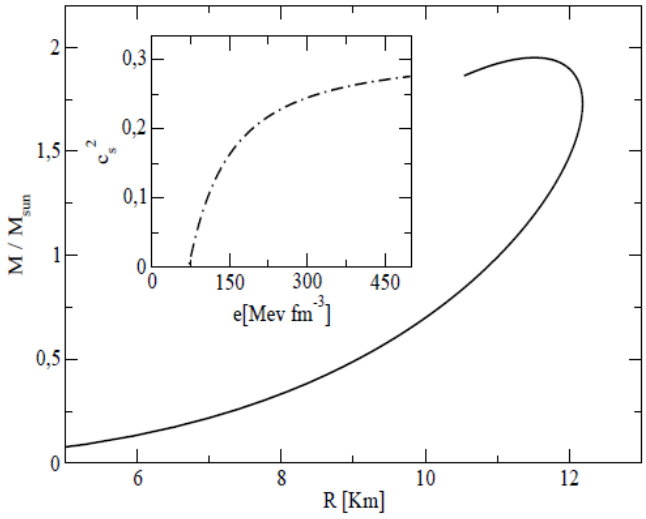

Prediction of the two families scenario on the fate of binary systems

Bauswein Stergioulas 2017

Four possible outcomes:

1) Prompt collapse (large masses)
2) Hypermassive (intermediate masses) living ~ few ms
3) Supramassive stars (living > few sec)
4) Stable stars

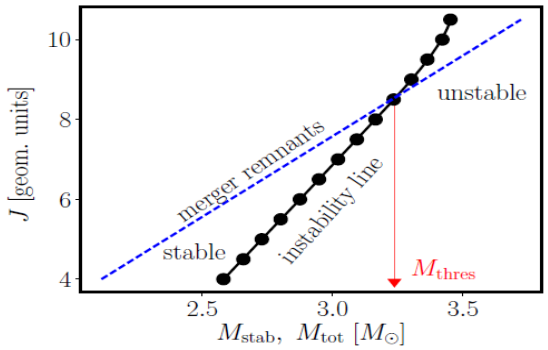

Figure 3. Angular momentum $J(M_{\rm stab})$ of differentially rotating NSs as function of the maximum stable mass $M_{\rm stab}$ for a given amount of angular momentum computed for the TM1 EoS (filled circles and solid line). The filled circles correspond to the sequence of turning points (axisymmetric instability line) in Fig 2, while the solid line is a fifth-order polynomial least-squares fit to the data. The dashed line represents the angular momentum in merger remnants $J_{\rm merger}(M_{\rm tot})$ as function of the total binary mass $M_{\rm tot}$. When $J_{\rm merger}(M_{\rm tot}) > J(M_{\rm stab})$ merger remnants are stable, otherwise they undergo prompt collapse to a black hole. The intersection $J_{\rm merger}(M_{\rm tot}) = J(M_{\rm stab})$ defines the threshold mass $M_{\rm thres}$ for prompt collapse.

Lecture of Bauswein:

At fixed total mass, the outcome depends on the EoS. The mass above which a prompt collapse is obtained is a simple function of M_{TOV}

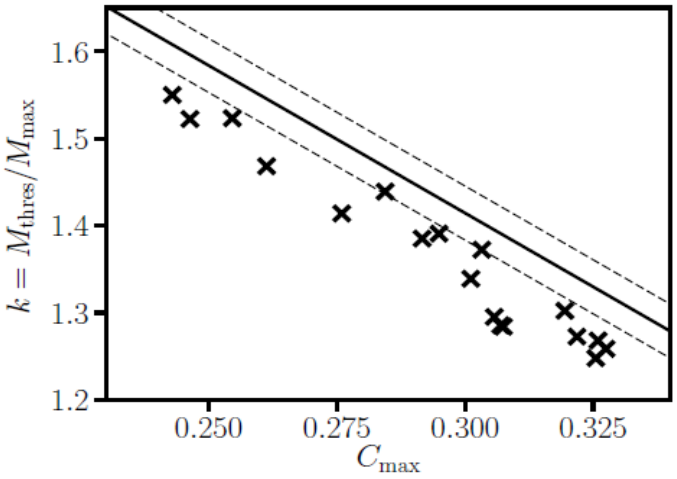

Key points of the two families scenario:

1) A merger would always produce at some stage a SS (stable or unstable) but for the case of the prompt collapse

2) In the cases of prompt collapse, the remnant collapses within t_c ~ few ms which is comparable with the time needed for the turbulent conversion of the hadronic star, t_{turb} (again few ms)

3) In the cases of prompt collapse the relevant M_{TOV} is not the maximum mass of SSs but the maximum mass of HSs which is in our scenario of the order of 1.5 - 1.6 M_{sun}

We expect therefore to have a large number of cases in which the prompt collapse occurs.

Bauswein et al 2016

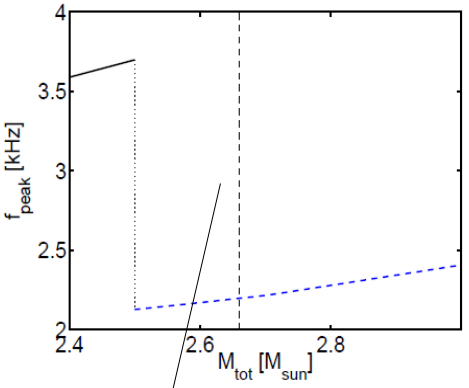

Fig. 17. Dominant postmerger GW frequency f_{peak} as a function of the total binary mass for symmetric mergers with a two-family scenario [46]. For low binary masses the merger remnant is composed of hadronuc matter (black curve), whereas higher binary masses lead to the formation of a strange matter remnant with a lower peak frequency (dashed blue curve). The vertical dashed line marks a lower limit on the binary mass which is expected to yield a remnant that is stable against gravitational collapse (see text).

For larger masses prompt collapse

By using the binary mass distribution from Kiziltan 2013 we can calculate the probabilites of prompt collapses in the two families scenario and in the one family scenario.

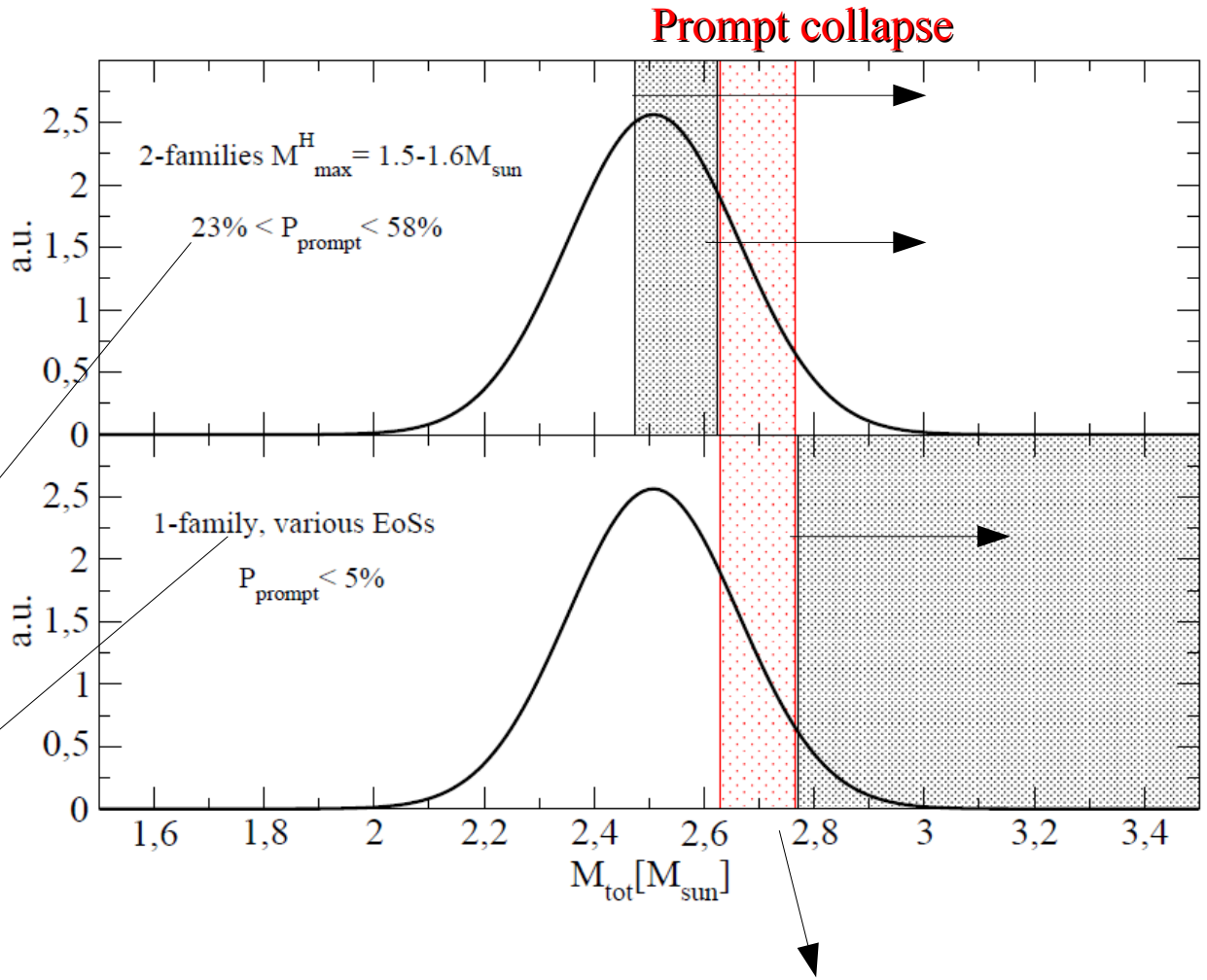

A clear separation of the expected probabilities: a prompt collapse “measured” from direct GW detection

A precise measurement of the total mass could distinguish between the two scenarios even with one (lucky) observation!

Analysis of the extendend emission of short GRBs

From the data one gets a lower limit of 22% of SGRB requiring a supramassive star and about 40 % of events in which a prompt collapse (including hypermassive stars) has occured.

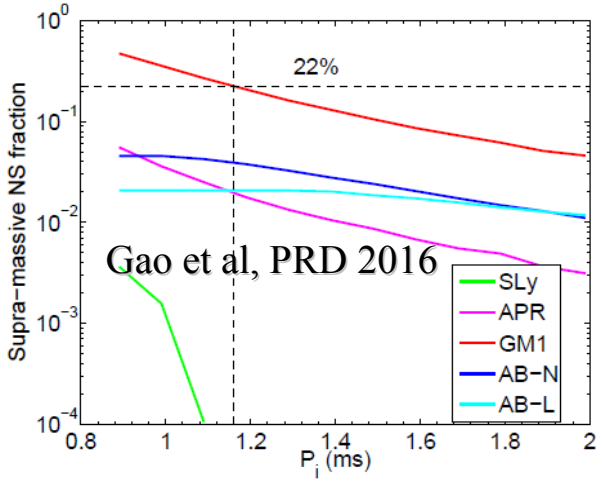

FIG. 1. Supra-massive NS formation fraction as a function of initial period for different EOSs. The distribution of NS masses are generated following the observationally-derived distribution of Galactic NS-NS systems, i.e. $M_{\rm BNS}$ has a normal distribution $N(\mu_{\rm BNS} = 1.32\,M_\odot, \sigma_{\rm BNS} = 0.11)$, with a mean $\mu_{\rm BNS}$ and a standard deviation $\sigma_{\rm BNS}$ [24].

Several hadronic equations of state "ruled out". Strange quark matter EOS are Ok. *Under the hypothesis that the extended emission is due to a protomagnetar (supramassive).*

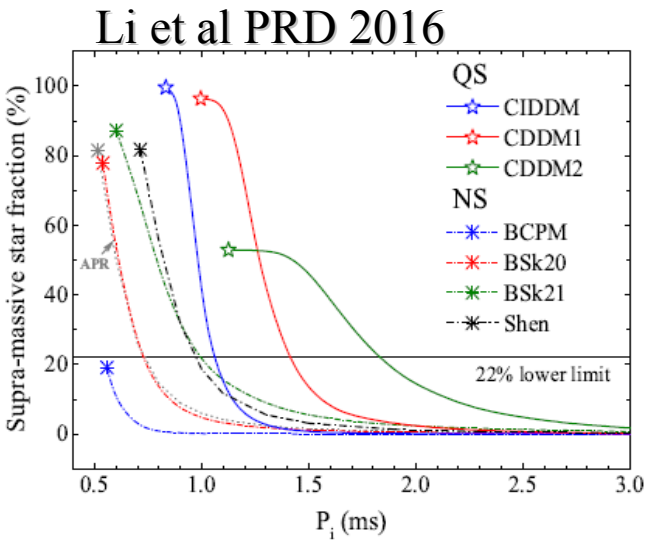

Deconfinement and the protomagnetar model of long GRB (Pili et al. 2016)

Conversion of rotating HSs

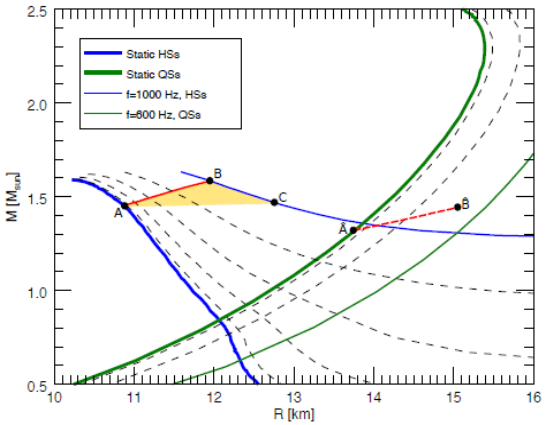

Figure 2. Gravitational mass as a function of the circumferential radius for both HSs and QSs. Thin dashed lines are sequences of stars at a fixed frequency from the non-rotating configurations (thick solid blue and green lines) to the configurations rotating at the maximum frequency (thin solid blue and green lines) and spaced by 200 Hz. The yellow region shows hadronic configurations centrifugally supported against deconfinement. Red lines and labels are the same as in figure 1.

Delayed deconfinement

Table 2. Spin-down timescales to start quark deconfinement Δt_{sd} together with the associated variation of the rotational kinetic energy ΔK_{sd} starting from an initial spin period P_i for the equilibrium sequences shown in figure 3. We also report the spin-down timescales Δt_q (defined as the time needed to half the rotational frequency of the QS) and the corresponding rotational energy loss ΔK_q after quark deconfinement. The initial magnetic field is of 10^{15} G.

M_0 [$M_\odot$]	$P_i \to P_d$ [ms]	Δt_{sd}	ΔK_{sd} [10^{52} erg]	Δt_q	ΔK_q [10^{52}erg]
1.666	$1.0 \to \infty$	∞	5.91	-	-
1.677	$1.0 \to 3.3$	2.7 hr	5.48	37 hr	0.19
	$2.0 \to 3.3$	1.8 hr	0.82		
	$3.0 \to 3.3$	37 min	0.13		
1.687	$1.0 \to 2.5$	1.5 hr	5.13	21 hr	0.33
	$2.0 \to 2.5$	36 min	0.46		
1.698	$1.0 \to 2.0$	55 min	4.68	14 hr	0.53
1.733	$1.0 \to 1.4$	23 min	3.37	8.2 hr	1.20
1.785	$1.0 \to 1.1$	6 min	1.37	5.4 hr	1.95
1.820	$1.0 \to 1.0$	0	0	4.6 hr	2.41

Many examples of "double bursts" in the LGRB data

UNUSUAL CENTRAL ENGINE ACTIVITY IN THE DOUBLE BURST GRB 110709B

Bin-Bin Zhang[1], David N. Burrows[1], Bing Zhang[2], Peter Mészáros[1,3], Xiang-Yu Wang[4,5], Giulia Stratta[6,7], Valerio D'Elia[6,7], Dmitry Frederiks[8], Sergey Golenetskii[8], Jay R. Cummings[9,10], Jay P. Norris[11], Abraham D. Falcone[1], Scott D. Barthelmy[12], Neil Gehrels[12]

Draft version June 24, 2013

ABSTRACT

The double burst, GRB 110709B, triggered *Swift*/BAT twice at 21:32:39 UT and 21:43:45 UT, respectively, on 9 July 2011. This is the first time we observed a GRB with two BAT triggers. In this paper, we present simultaneous *Swift* and Konus-*WIND* observations of this unusual GRB and its afterglow. If the two events originated from the same physical progenitor, their different time-dependent spectral evolution suggests they must belong to different episodes of the central engine, which may be a magnetar-to-BH accretion system.

Subject headings: gamma-ray burst: general

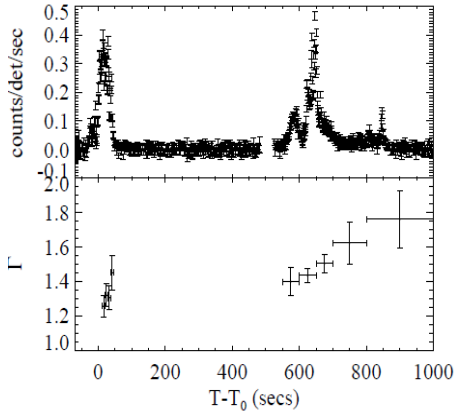

GWs within the two families scenario

If the postmerger signal will be measured: the two families scenario would predict a jump in the value of f_{peak} for increasing total mass.

Bauswein et al 2016

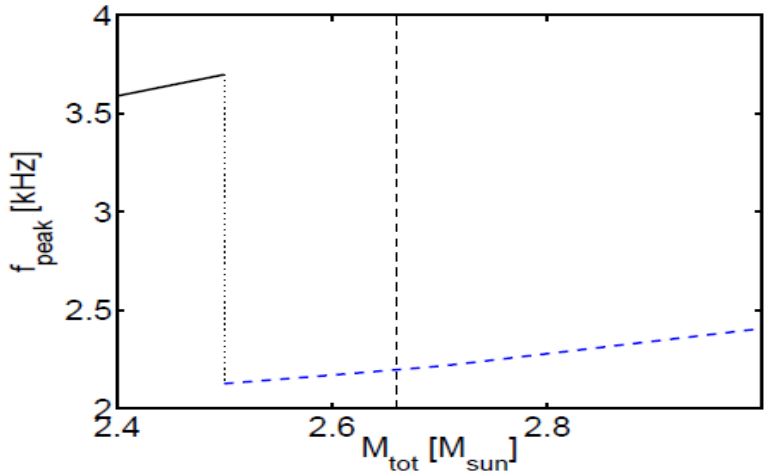

Fig. 17. Dominant postmerger GW frequency f_{peak} as a function of the total binary mass for symmetric mergers with a two-family scenario [46]. For low binary masses the merger remnant is composed of hadronuc matter (black curve), whereas higher binary masses lead to the formation of a strange matter remnant with a lower peak frequency (dashed blue curve). The vertical dashed line marks a lower limit on the binary mass which is expected to yield a remnant that is stable against gravitational collapse (see text).

Conclusions

-) The conversion of a hadronic star into a quark star proceeds via two steps: turbulent regime (time scale ms) – diffusive regime (10 s)

-) Burst of neutrinos with an extended tail

-) New masses and radii measurements challenge nuclear physics: tension between high mass and small radii. 2.45 M_{sun} candidates already exist.

-) NICER, LOFT, Athena+, GAIA missions, with a precision of 1km in radii measurements, could hopefully solve the problem.

-) Possible existence of two families of compact stars (high mass – quark stars, low mass – hadronic stars). Rich phenomenolgy: frequency distributions, moment of inertia, explosive events, quark stars are the necessary compact remnants formed during NS mergers (if a BH is not formed promptly).

Working with us

-) 2 PhD positions in our deparmenent for foreigners

http://www.unife.it/studenti/dottorato/concorsi/selection

-) 1 INFN post-doc on theoretical physics *(coming soon)*

Appendix

Do we have any experimental/theoretical information on $x_{\omega\Delta}$ & $x_{\sigma\Delta}$?

Electron, pion scattering photoabsorption on nuclei (O'Connel et al 1990, Wehrberger et al1989...). Indications of a Δ potential in the nuclear medium deeper than the nucleon potential. Several phenomenological and theoretical analyses lead to similar conclusions.

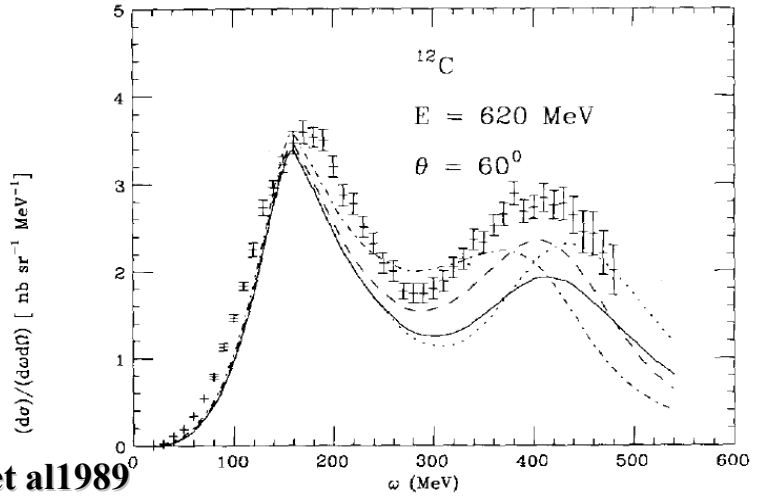

Wehrberger et al1989

Fig. 13. Cross section for electron scattering on ^{12}C at incident electron energy $E = 620$ MeV and scattering angle $\theta = 60°$ as a function of energy transfer ω for standard nucleon and different Δ-couplings. The lines are the results for the sum of the contribution from nucleon knockout and Δ-excitation. The dotted line shows the cross section for free Δ's, and the dashed and dot-dashed lines for no coupling to the vector field and a ratio $r_s = 0.15$ and 0.30 of the scalar coupling of the Δ to the scalar coupling of the nucleon. The solid line is obtained for universal coupling. The data are from ref. [16]).

Phenomenological potentials:

$$\omega = E_f - E_i$$

$$= (p_f^2 + W^2)^{1/2} + V_W(p_f) - (p_i^2 + M^2)^{1/2} - V_N(p_i)$$

$$V(p) = -V_0/(1 + p^2/p_0^2) + V_1$$

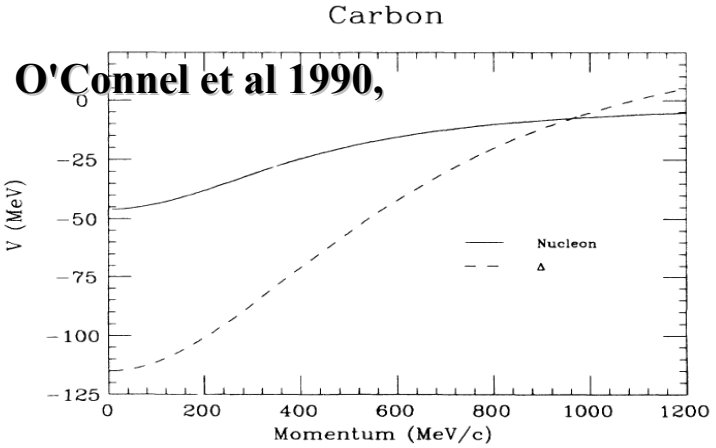

O'Connel et al 1990,

FIG. 4. Phenomenological nucleon-nucleus, solid line, and Δ nucleus, dashed line, momentum-dependent potentials for C.

This allows to constrain the free parameters within the RMF model. Notice: coupling with ω mesons suppressed wrt the coupling with the σ meson.
The coupling(ratio) with the ρ meson fixed to 1.

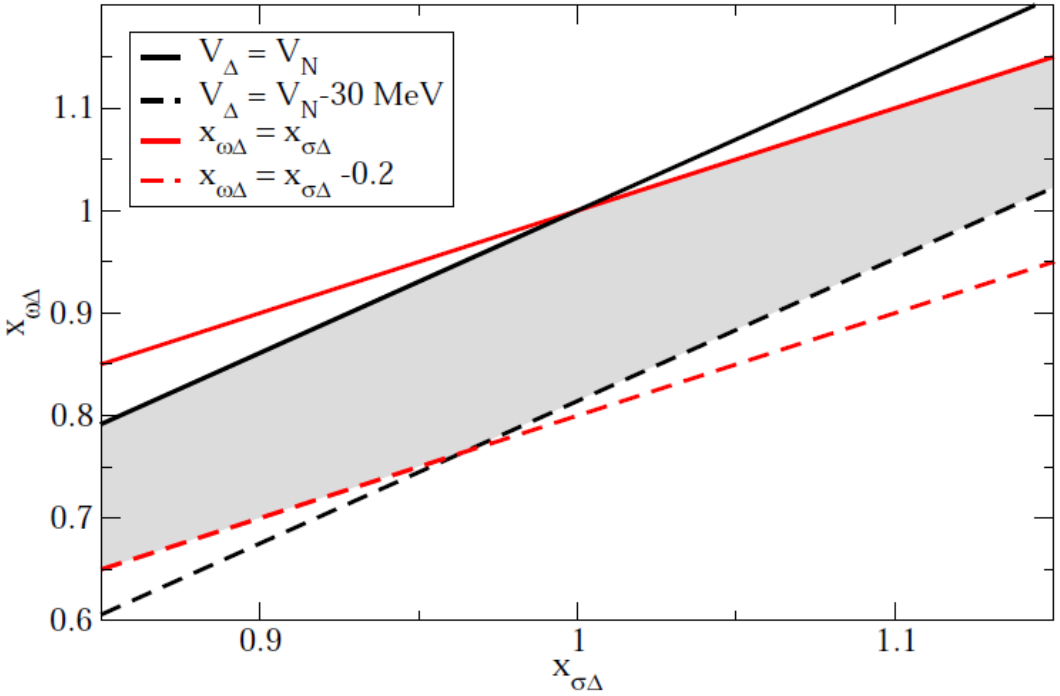

Implications for compact stars ?

Maximum mass and radii: the maximum mass is significantly smaller than the measured ones. Also, very compact stellar configurations are possible.

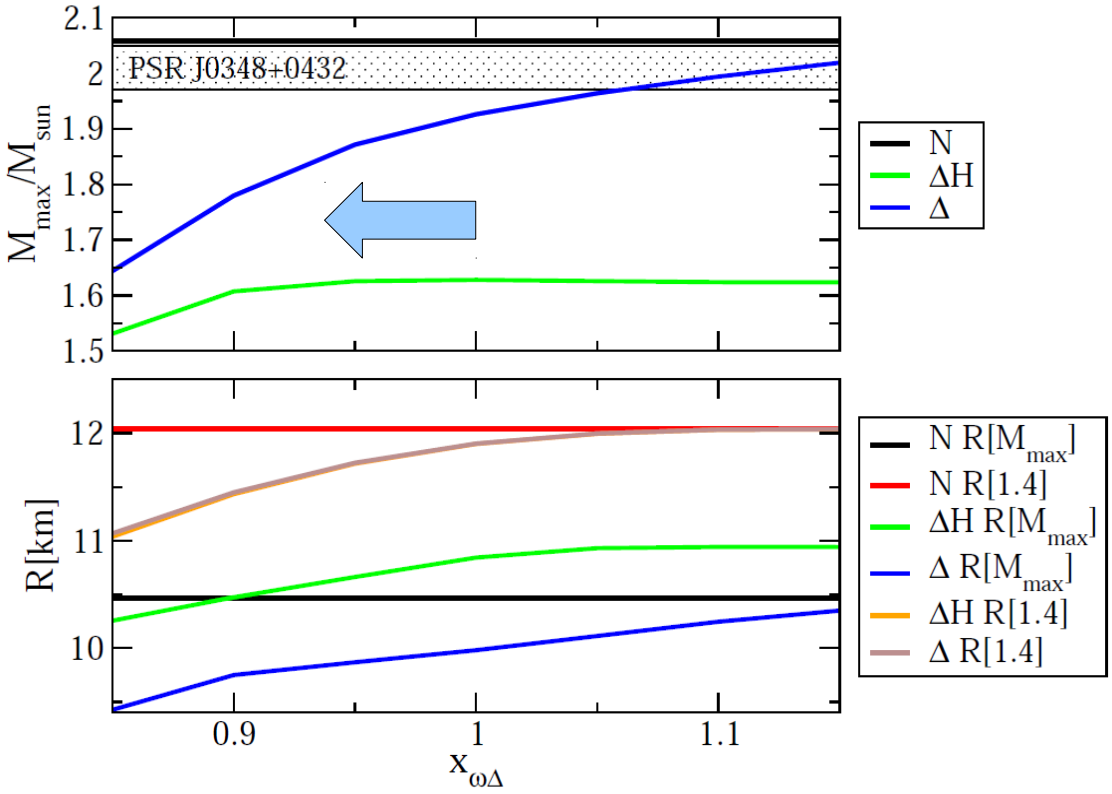

See also:

(Schurhoff, Dexheimer, Schramm 2010)

Punchline/?: beside the "hyperon puzzle" is there also a "delta isobars puzzle"?

To do: include the imaginary part of the delta self-energy in the equation of state calculations.

Simple estimates with a Breit-Wigner-like distribution. Critical density within the range of neutron stars central densities.

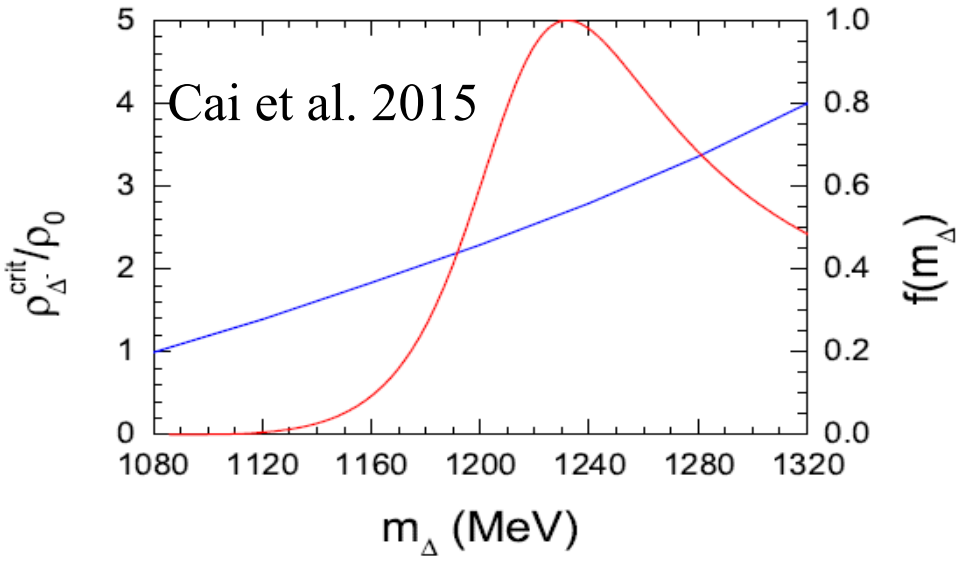

Figure 3: (Color Online) The Delta mass m_Δ dependence of the critical density $\rho_{\Delta^-}^{\rm crit}$ for Δ^- formation in neutron stars (blue) and the Breit-Wigner mass distribution of Delta resonances in free-space (red).

$$f(m_\Delta) = \frac{1}{4}\frac{\Gamma^2(m_\Delta)}{(m_\Delta - m_\Delta^0)^2 + \Gamma^2(m_\Delta)/4}$$

… dramatic results in microscopic calculations

Hyperons puzzle: *"…the treatment of hyperons in neutron stars is necessary and any approach to dense matter must address this issue."*

The solution is not just the "let's use only nucleons"

Vidana et al 2011

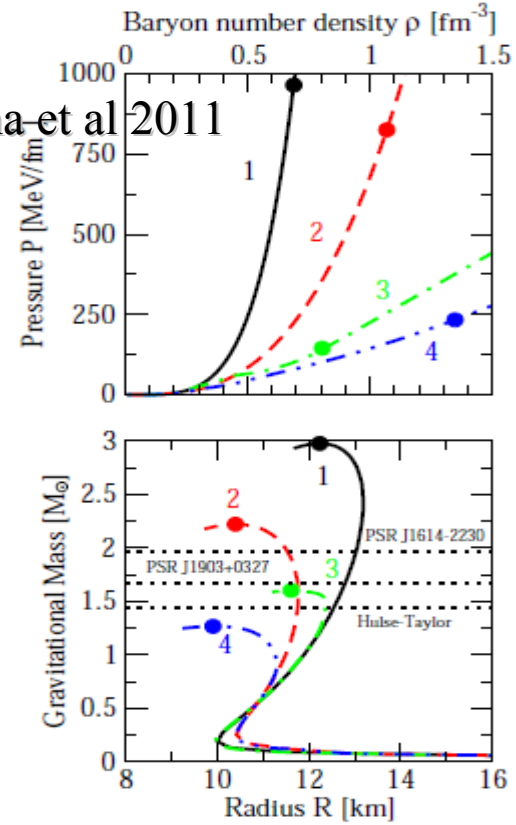

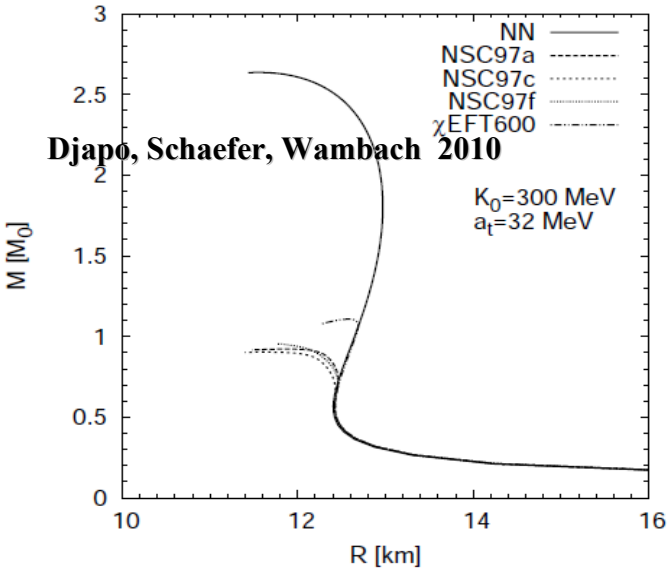

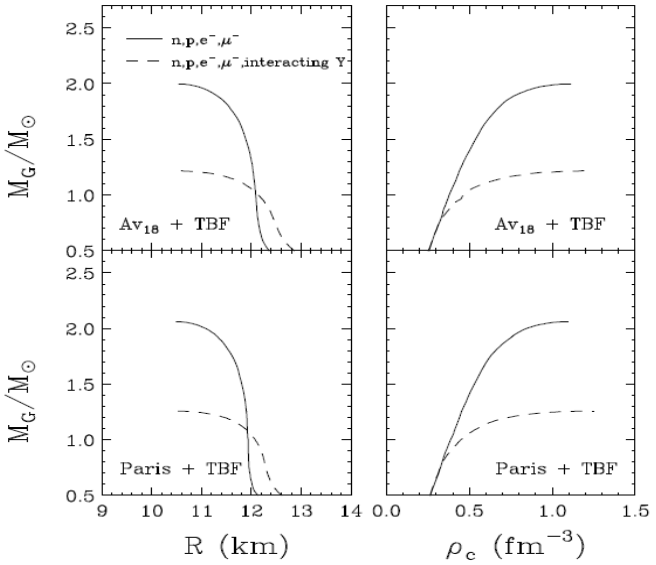

Baldo et al 1999

What about delta resonances?

Symmetry energy: the L parameter
(see talk of M. Colonna)

Symmetry energy and its density derivative

$$e(n,x) = e(n,1/2) + S_2(n)(1-2x)^2 + \ldots$$

$$S_v = S_2(n_s),$$

$$L = 3n_s(dS_2/dn)_{n_s}$$

Lattimer et al 2013

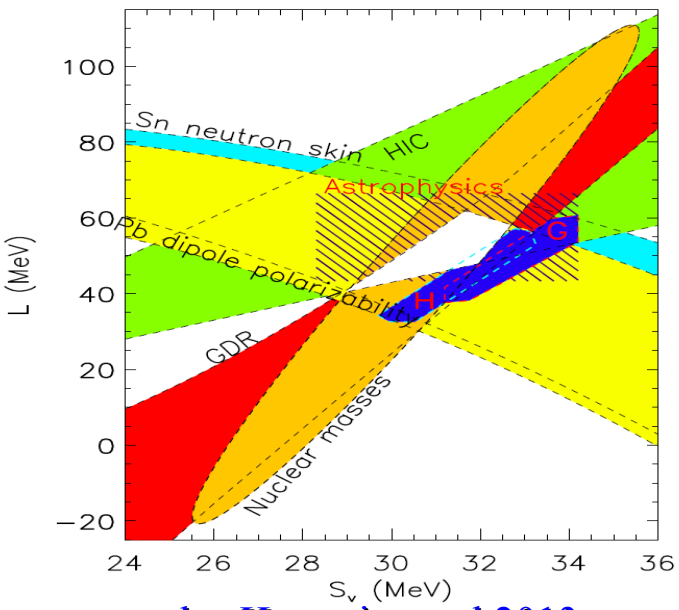

see also Horowitz et al 2013

Within the old Glendenning mean field parametrizations it was not possible to include this parameter as an additional constraint on nuclear matter

NEUTRON STARS ARE GIANT HYPERNUCLEI?[1]

NORMAN K. GLENDENNING
Nuclear Science Division, Lawrence Berkeley Laboratory, University of California, Berkeley
Received 1984 March 28; accepted 1984 December 3

$$\mathcal{L} = \sum_B \bar{B}(i\gamma_\mu \partial^\mu - m_B + g_{\sigma B}\sigma - g_{\omega B}\gamma_\mu \omega^\mu)B$$

$$- g_\rho \rho_{\mu 3} J_3{}^\mu + \mathcal{L}_\sigma{}^0 + \mathcal{L}_\omega{}^0 + \mathcal{L}_\rho{}^0 + \mathcal{L}_\pi{}^0 - U(\sigma)$$

$$U(\sigma) = [bm_N + c(g_\sigma \sigma)](g_\sigma \sigma)^3$$

Only S_v could be fixed through g_ρ

… it turns out that in the GM1-2-3 parametrizations L ~ 80 MeV thus higher than the values indicated by the recent analysis of Lattimer & Lim.

Baryons thresholds equation

(see talk of Providencia):

$$\mu_n - q_B \mu_e \geq g_{\omega B}\,\omega_0 + g_{\rho B}\,\rho_{03}\,I_{3B} + m_B - g_{\sigma B}\,\sigma$$

Disfavours the appearance of particles, such as Δ^- , with negative isospin charge. Δ^- could form in beta-stable matter only if g_ρ is set =0 (Glendenning 1984).

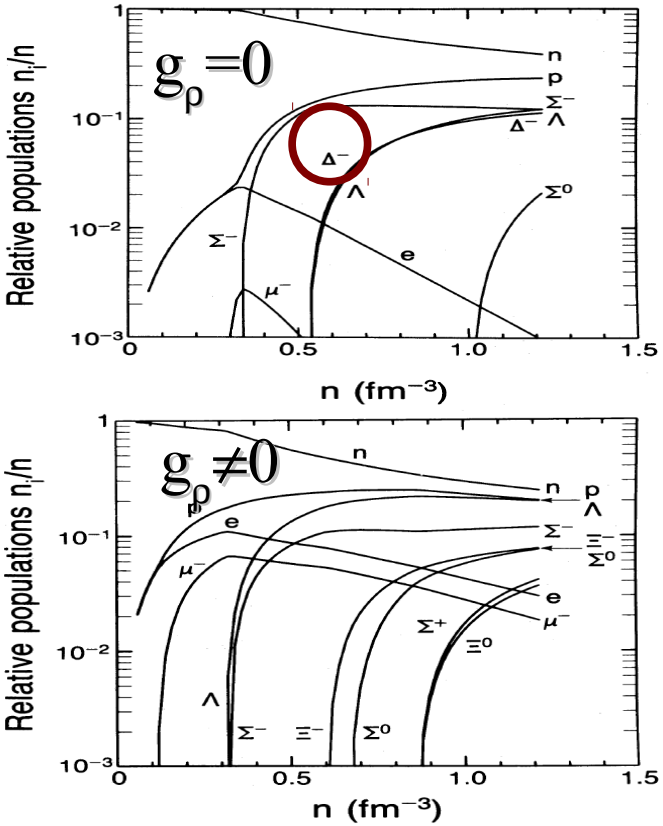

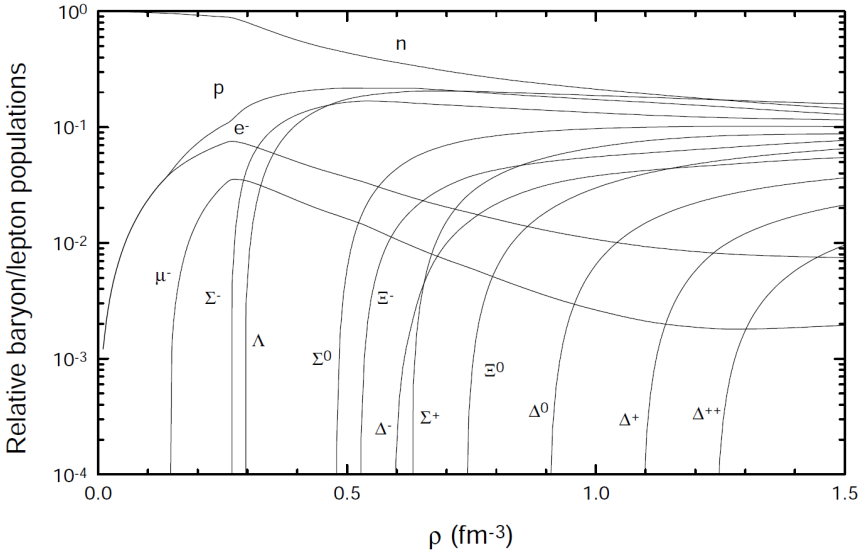

Δ^- easier to form in RHF calculations (see Huber et al 1998) due to the smaller value of g_ρ

A toy model: introduce a density dependence of g_ρ within the GM3 model (density dependence as in Typel et al 2009)

$$f_i(x) = \exp[-a_i(x-1)]$$

The additional parameter "a" allow to fix L. Coupling ratios =1 for Δ, for hyperons potential depths and flavor symmetry (Schaffner 2000).

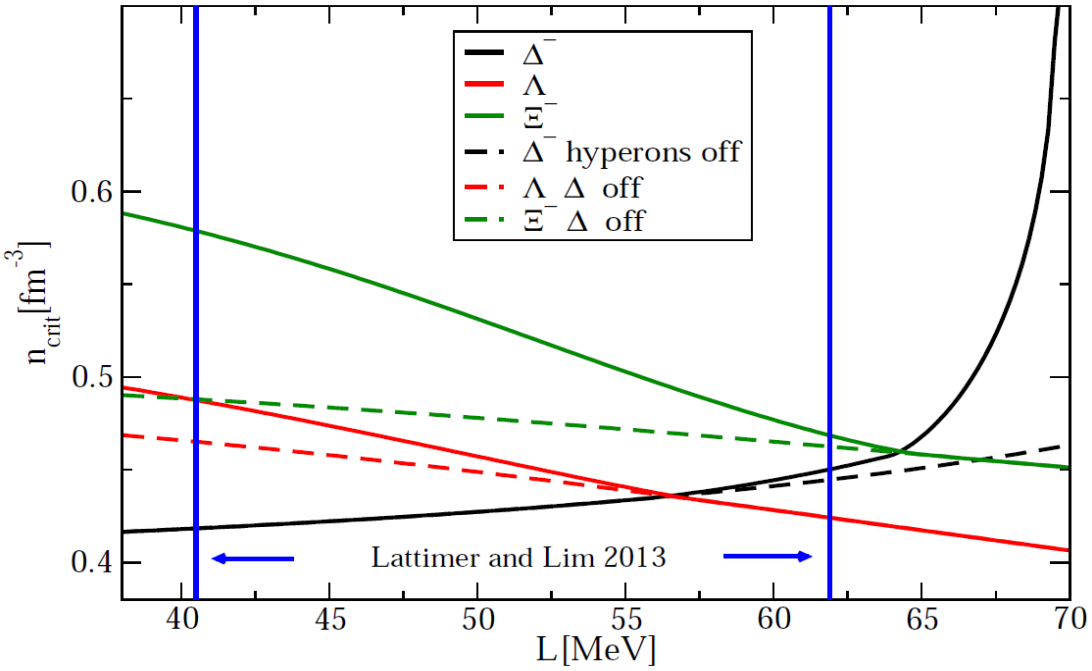

Glendenning's results

Different behaviour of the hyperons and Δ thresholds as functions of L:

$$g_{\rho n}\rho + \sqrt{k_{Fn}^2 + m_n^{*2}} + \mu_e = m_{\Delta^-}^*$$

Punch line: for the range of L indicated by Lattimer & Lim, Δ appear already at 2-3 saturation density, thus comparable to the density of appearance of hyperons. If Δ form before hyperons, hyperons are shifted to higher densities (w.r.t. the case of no Δ)

The recent SFHo model (Steiner et al 2013): additional terms added to better exploit the experimental information

$$\mathcal{L} = \bar{\Psi}\left[i\partial\!\!\!/ - g_\omega \omega\!\!\!/ - \tfrac{1}{2} g_\rho \vec{\rho}\!\!\!/ \cdot \vec{\tau} - M + g_\sigma \sigma - \tfrac{1}{2} e\,(1+\tau_3)\, A\!\!\!/\right]\Psi + \tfrac{1}{2}\,(\partial_\mu \sigma)^2$$
$$-V(\sigma) - \tfrac{1}{4} f_{\mu\nu} f^{\mu\nu} + \tfrac{1}{2} m_\omega^2 \omega^\mu \omega_\mu - \tfrac{1}{4} \vec{B}_{\mu\nu} \cdot \vec{B}^{\mu\nu} + \tfrac{1}{2} m_\rho^2 \vec{\rho}^{\,\mu} \cdot \vec{\rho}_\mu - \tfrac{1}{4} F_{\mu\nu} F^{\mu\nu}$$
$$+\frac{\zeta}{24} g_\omega^4 \left(\omega^\mu \omega_\mu\right)^2 + \frac{\xi}{24} g_\rho^4 \left(\vec{\rho}^{\,\mu} \cdot \vec{\rho}_\mu\right)^2 + g_\rho^2 f(\sigma, \omega_\mu \omega^\mu) \vec{\rho}^{\,\mu} \cdot \vec{\rho}_\mu$$,Steiner et al 2005

PROPERTIES AT SATURATION DENSITY AND NEUTRON STAR PROPERTIES FOR THE THE DIFFERENT EOSS UNDER INVESTIGATION. THE DEFINITION OF ALL THE QUANTITIES IS GIVEN IN THE TEXT.

EOS	n_B^0 [fm^{-3}]	E_0 [MeV]	K [MeV]	K' [MeV]	J [MeV]	L [MeV]	m_n^*/m_n -	m_p^*/m_p -	$R_{1.4}$ [km]	$M_{T=0,Max}$ [$M_\odot$]	$M_{s=4,Max}$ [$M_\odot$]
SFHo	0.1583	16.19	245.4	-467.8	31.57	47.10	0.7609	0.7606	11.88	2.059	2.27
SFHx	0.1602	16.16	238.8	-457.2	28.67	23.18	0.7179	0.7174	11.97	2.130	2.36
STOS(TM1)	0.1452	16.26	281.2	-285.3	36.89	110.79	0.6344	0.6344	14.56	2.23	2.62
HS(TM1)	0.1455	16.31	281.6	-286.5	36.95	110.99	0.6343	0.6338	13.84	2.21	2.59
HS(TMA)	0.1472	16.03	318.2	-572.2	30.66	90.14	0.6352	0.6347	14.44	2.02	2.48
HS(FSUgold)	0.1482	16.27	229.5	-523.9	32.56	60.43	0.6107	0.6102	12.52	1.74	2.34
LS(180)	0.1550	16.00	180.0	-450.7	28.61	73.82	1	1	12.16	1.84	2.02
LS(220)	0.1550	16.00	220.0	-411.2	28.61	73.82	1	1	12.62	2.06	2.14

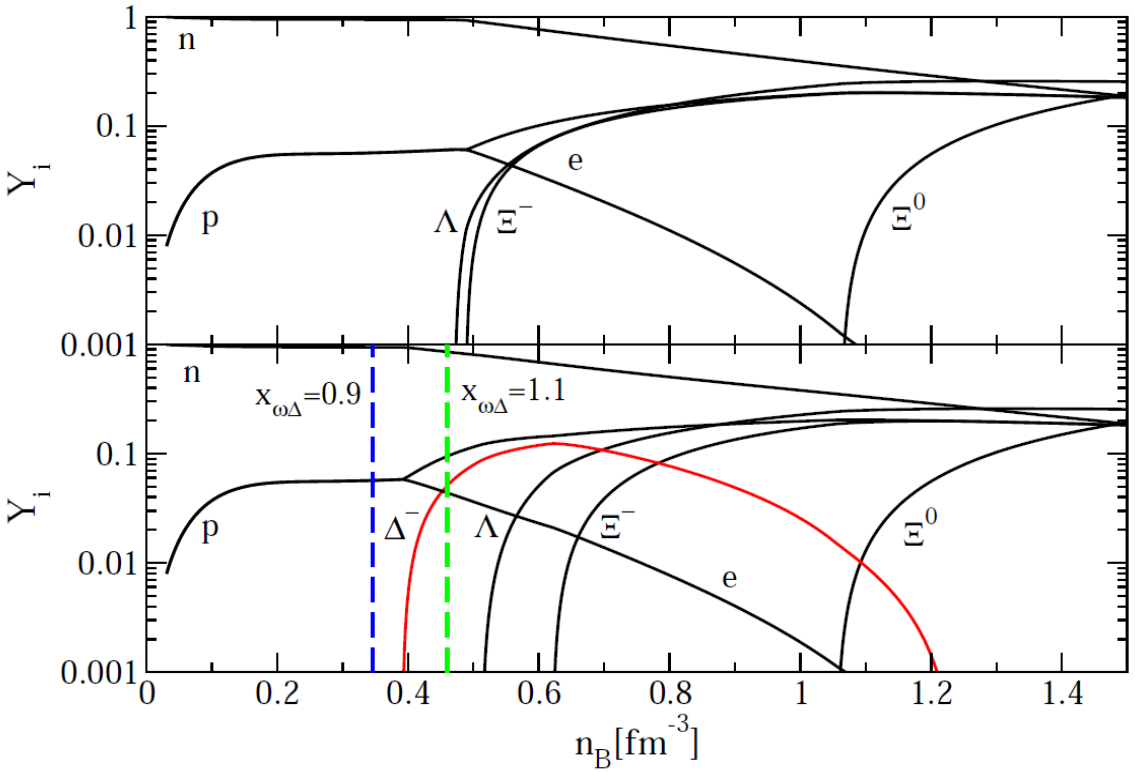

Introducing both hyperons and Δ in the SFHo model: Δ appear before hyperons even in the case of $x_{\omega\Delta} > 1$.

What prevents the conversion of a metastable hadronic star?

A star containing only nucleons and Δ cannot convert into a quark star because of the lack of strangeness (need for multipole simultaneous weak interactions).
Only when hyperons start to form the conversion can take place.

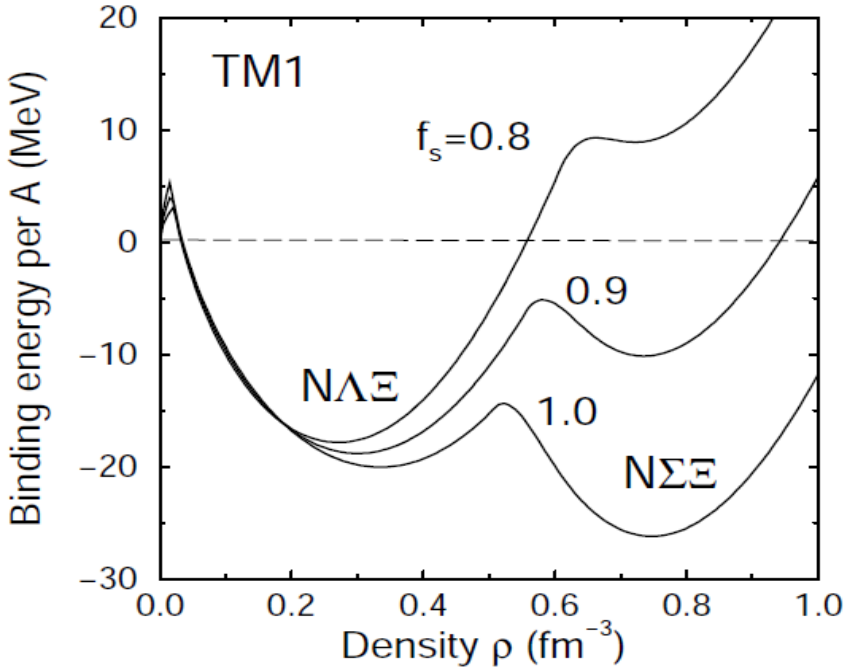

New minima of BE/A could appear when increasing strangeness, (very) strange hypernuclei (Schaffner-Bielich- Gal 2000)

Within a simple parametrization:

$$\Omega_{QM} = \sum_{i=u,d,s,e} \Omega_i + \frac{3\mu^4}{4\pi^2}(1-a_4) + B_{eff}$$

Two EoSs which provide a maximum mass of $2M_{sun}$

- E/A=860 MeV(set1)
- E/A=930 MeV(set2)

Different QSs binding energy M_B-M_G

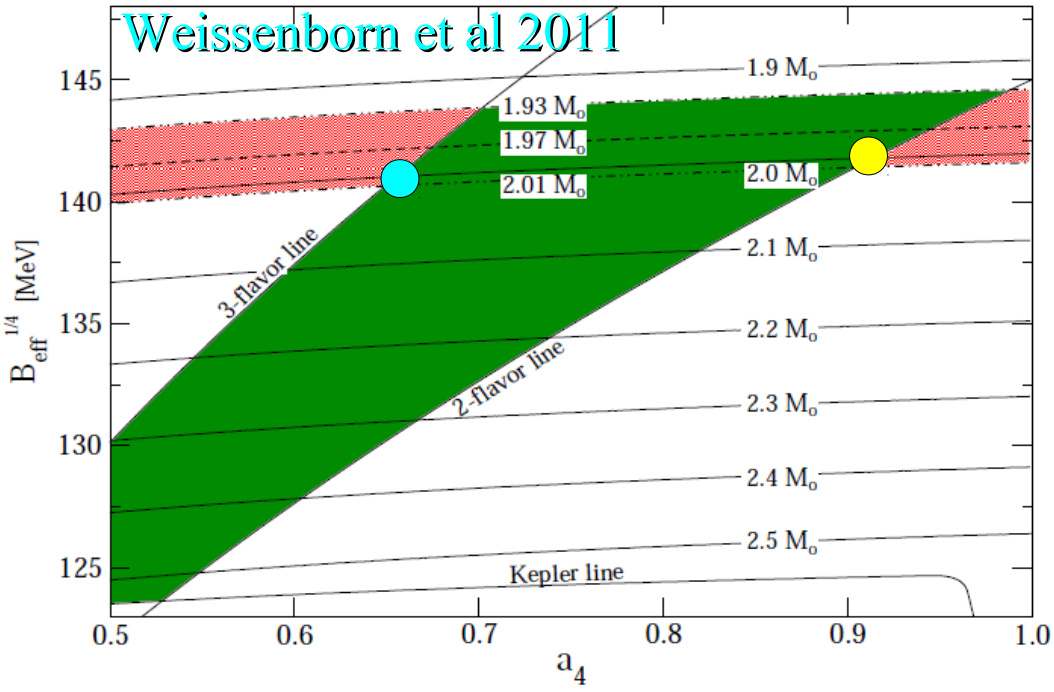

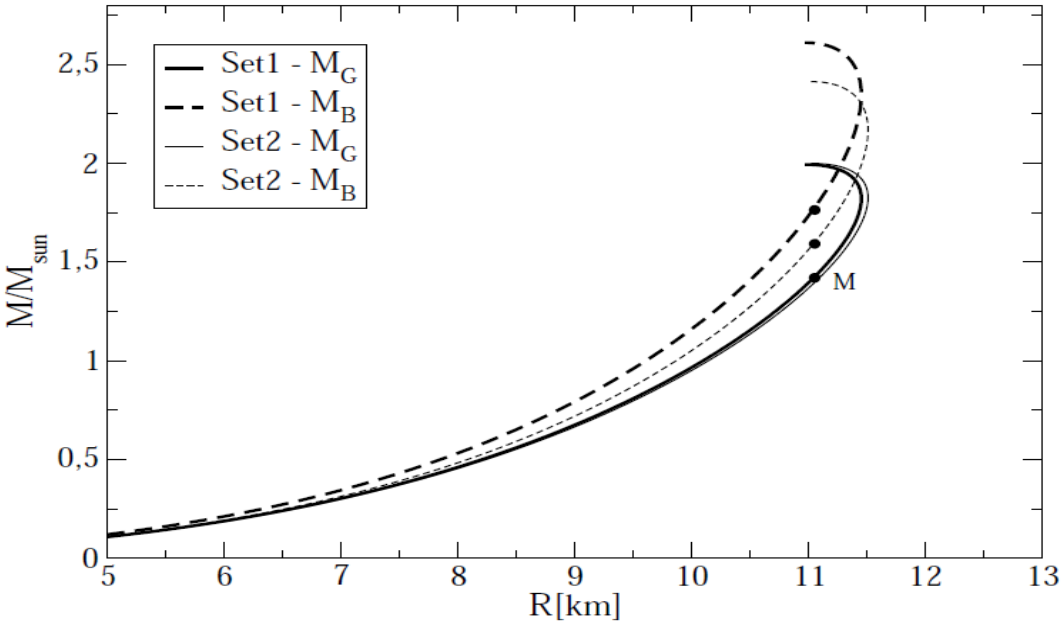

… is this surprising?

Also at finite density the quark matter equation of state should be stiffer than the hadronic equation of state in which new particles are produced as the density increases

Heavy ions physics: (Kolb & Heinz 2003)

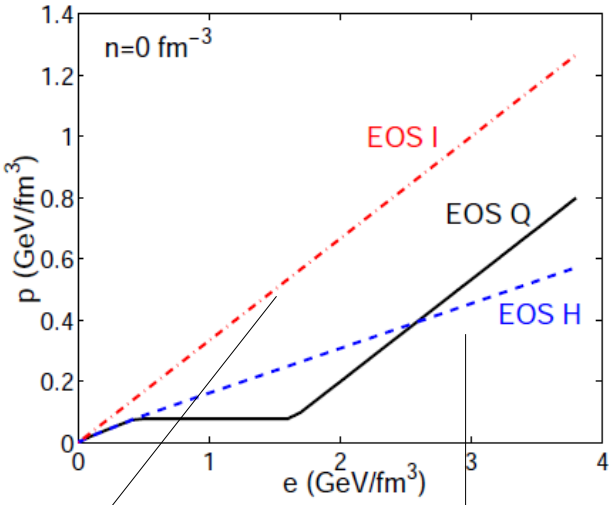

Fig. 1. Equation of state of the Hagedorn resonance gas (EOS H), an ideal gas of massless particles (EOS I) and the Maxwellian connection of those two as discussed in the text (EOS Q). The figure shows the pressure as function or energy density at vanishing net baryon density.

p=e/3 massless quarks

Hadron resonance gas p=e/6

Why conversion should then occur? Quark stars are more bound: at a fixed total baryon number they have a smaller gravitational mass wrt hadronic stars

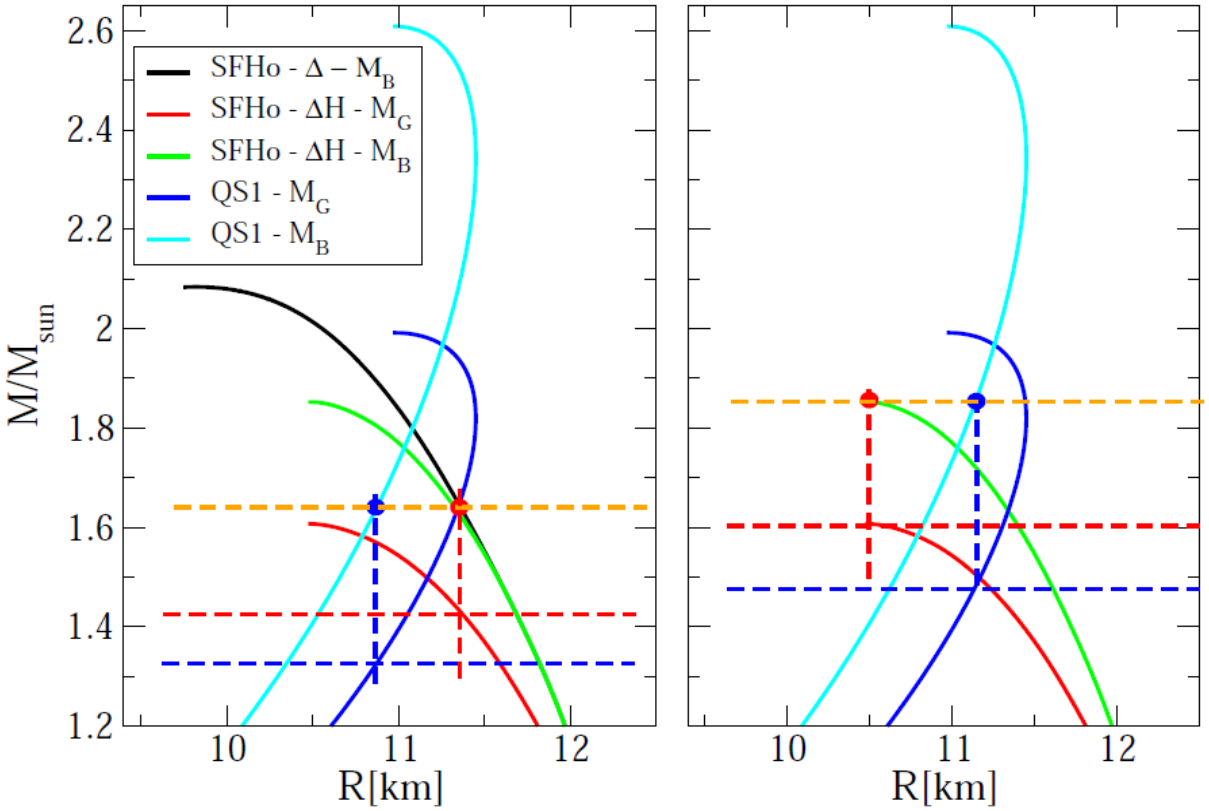

Are all compact stars strange?: Merger of strange stars

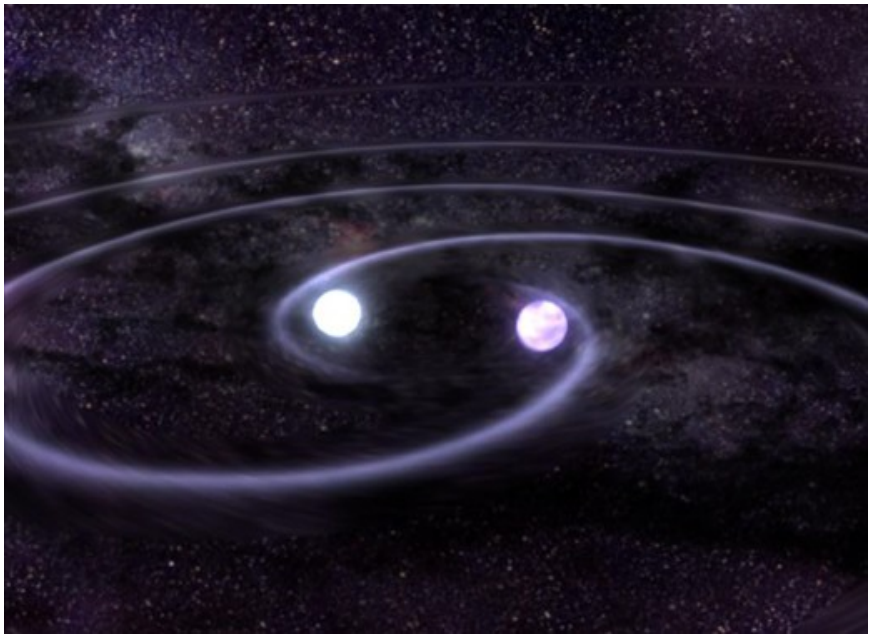

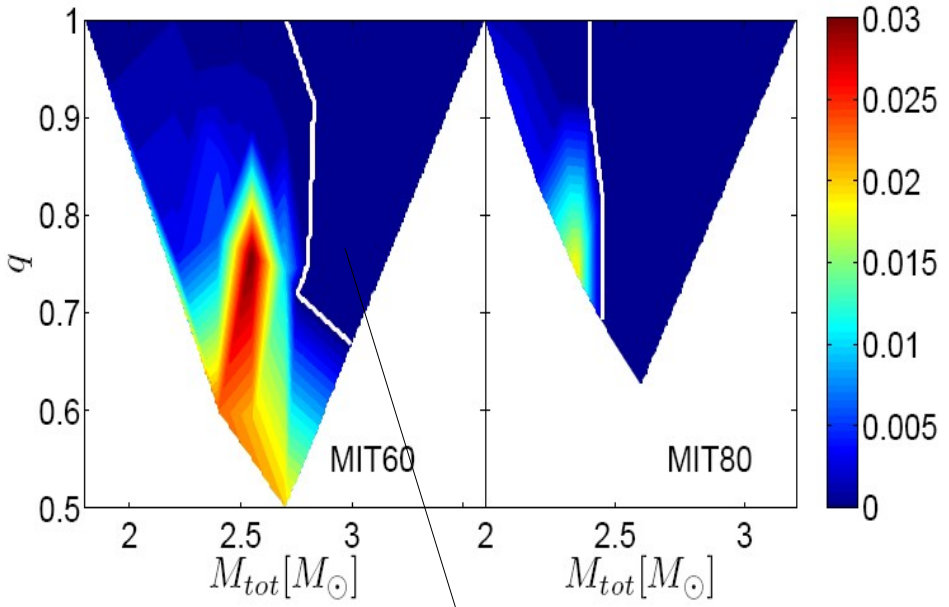

MIT60: 8 10^{-5} M_{sun}, MIT80 no ejecta. By assuming a galactic merger rate of $10^{-4(-5)}$/year, mass ejected: $10^{-8(-9)}$ M_{sun}/year. Constraints on the strangelets flux (for AMS02)

A. Bauswein et al PRL (2009)

Prompt collapse: in our scenario quark stars have masses larger than ~ 1.5 M_{sun}, no strangelets emitted.

Hyperons in compact stars

Few experimental data from hypernuclei: potential depths of Λ, Σ, Ξ allow to fix three parameters (usually the coupling with a scalar meson).

Within RMF:

(see Weissenborn, Chatterjee, Schaffner-Bielich 2012)

$$\mathcal{L} = \sum_B \bar{\Psi}_B \left(i\gamma_\mu \partial^\mu - m_B + g_{\sigma B}\sigma - g_{\omega B}\gamma_\mu \omega^\mu - g_{\rho B}\gamma_\mu \mathbf{t}_B \cdot \boldsymbol{\rho}^\mu \right) \Psi_B$$
$$+ \frac{1}{2}\left(\partial_\mu \sigma \partial^\mu \sigma - m_\sigma^2 \sigma^2 \right) - U(\sigma) + U(\omega)$$
$$- \frac{1}{4}\omega_{\mu\nu}\omega^{\mu\nu} + \frac{1}{2}m_\omega^2 \omega_\mu \omega^\mu - \frac{1}{4}\boldsymbol{\rho}_{\mu\nu} \cdot \boldsymbol{\rho}^{\mu\nu} + \frac{1}{2}m_\rho^2 \boldsymbol{\rho}_\mu \cdot \boldsymbol{\rho}^\mu .$$

$$\mathcal{L}_{YY} = \sum_B \bar{\Psi}_B \left(g_{\sigma^* B}\sigma^* - g_{\phi B}\gamma_\mu \phi^\mu \right) \Psi_B$$
$$+ \frac{1}{2}\left(\partial_\mu \sigma^* \partial^\mu \sigma^* - m_{\sigma^*}^2 \sigma^{*2} \right)$$
$$- \frac{1}{4}\phi_{\mu\nu}\phi^{\mu\nu} + \frac{1}{2}m_\phi^2 \phi_\mu \phi^\mu .$$

Additional YY interaction

$$\frac{1}{3}g_{\omega N} = \frac{1}{2}g_{\omega \Lambda} = \frac{1}{2}g_{\omega \Sigma} = g_{\omega \Xi},$$
$$g_{\rho N} = \frac{1}{2}g_{\rho \Sigma} = g_{\rho \Xi},$$
$$g_{\rho \Lambda} = 0,$$
$$2g_{\phi \Lambda} = 2g_{\phi \Sigma} = g_{\phi \Xi} = -\frac{2\sqrt{2}}{3}g_{\omega N}.$$

Couplings with vector mesons from flavor symmetry

Particle's fractions

Beta stable matter (equilibrium with respect to weak interaction+charge neutrality): large isospin asymmetry and large strangeness , very different from the nuclear matter produced in heavy ions collisions

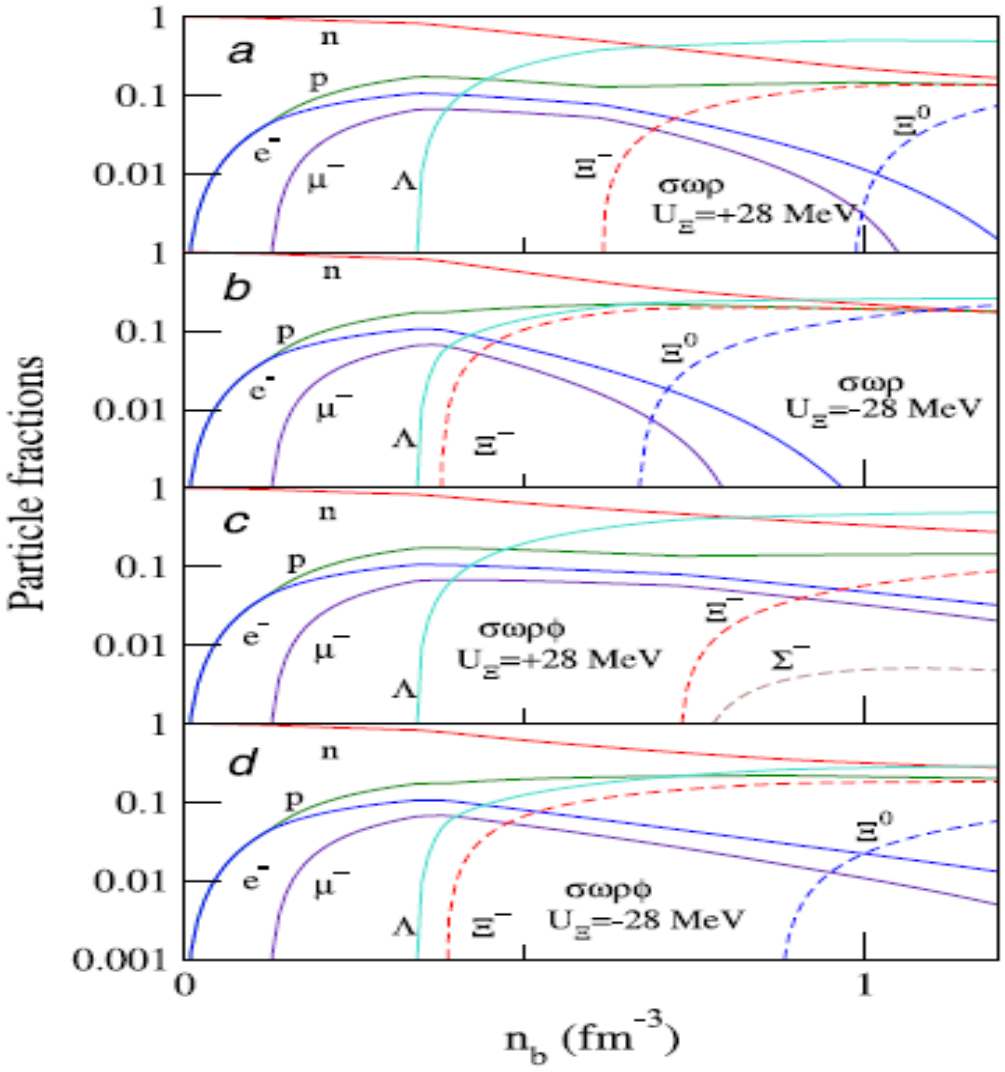

Notice: hyperons appear at 2-3 times saturation density

The appearance of hyperons sizably softens the equation of state: reduced maximum mass

Introducing the ϕ meson to obtain YY repulsion allows to be marginally consistent with the astrophysical data.

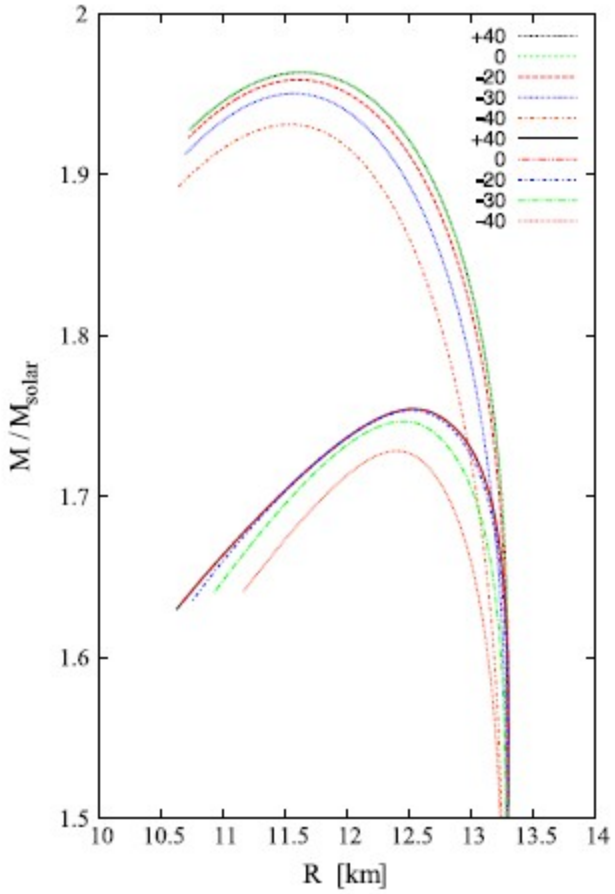

Fig. 2. Mass radius relations for neutron stars obtained with the EoS from Fig. 1. The variation of $U_\Sigma^{(N)}$ in "model $\sigma\omega\rho$" cannot account for the observed neutron star mass limit (lower branch), unless the ϕ meson is included in the model (upper branch).

… but: σ* (to be interpreted as the f0(980)) has not been included. Introducing this additional interaction would again reduce the maximum mass

What about Δ?

Here only Δ are included

Similar effects: softening of the equation of state. Just small changes of the couplings with vector mesons sizably decrease the maximum mass

(Schurhoff, Dexheimer, Schramm 2010)

Notice: very small radii

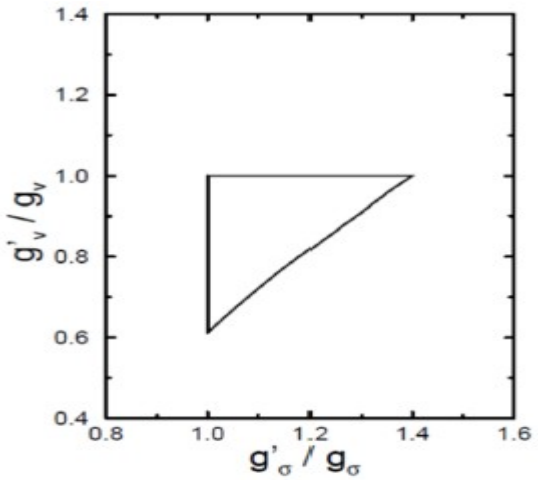

Kosov, Fuchs, Marmyanov, Faessler, PLB 421 (1998) 37

Some constraints on the couplings with mesons from nuclear matter properties and QCD sum rules

Temperature profiles as initial conditions for the cooling diffusion equation

Assumption: quark matter is formed already in beta equilibrium, no lepton number conservation imposed in the burning simulation, no lepton number diffusion

Diffusion is dominated by scattering of non-degenenerate neutrinos off degenerate quarks

$$\frac{\sigma_S}{V} = \frac{G_F^2 E_\nu^3 \mu_i^2}{5\pi^3}$$

Steiner et al 2001

Heat transport equation due to neutrino diffusion

$$\frac{\mathrm{d}}{\mathrm{dt}}\frac{\epsilon_{tot}}{n_b} + P\frac{\mathrm{d}}{\mathrm{dt}}\frac{1}{n_b} = -\frac{\Gamma}{n_b r^2 \mathrm{e}^{\Phi}}\frac{\partial}{\partial r}\left(\mathrm{e}^{2\Phi} r^2 \left(F_{\epsilon,\nu_e} + F_{\epsilon,\nu_\mu}\right)\right)$$

$$\frac{dP}{dr} = -(P+\epsilon_{tot})\frac{m+4\pi r^3 P}{r^2-2mr}$$

$$\frac{dm}{dr} = 4\pi r^2 \epsilon_{tot}$$

$$\frac{da}{dr} = \frac{4\pi r^2 n_b}{\sqrt{1-2m/r}}$$

$$\frac{d\Phi}{dr} = \frac{m+4\pi r^3 P}{r^2-2mr}$$

$$F_{\epsilon,\nu_e} = -\frac{\lambda_{\epsilon,\nu_e}}{3}\frac{\partial \epsilon_{\nu_e}}{\partial r}$$

$$F_{\epsilon,\nu_\mu} = -\frac{\lambda_{\epsilon,\nu_\mu}}{3}\frac{\partial \epsilon_{\nu_\mu}}{\partial r}$$

Expected smaller cooling times with respect to hot neutron stars

phase	process	λ(T=5 MeV)	λ(T=30 MeV)
Nuclear	$\nu n \to \nu n$	200 m	1 cm
Matter	$\nu_e n \to e^- p$	2 m	4 cm
Unpaired	$\nu q \to \nu q$	350 m	1.6 m
Quarks	$\nu d \to e^- u$	120 m	4 m
CFL	λ_{3B}	100 m	70 cm
	$\nu\phi \to \nu\phi$	>10 km	4 m

Reddy et al 2003

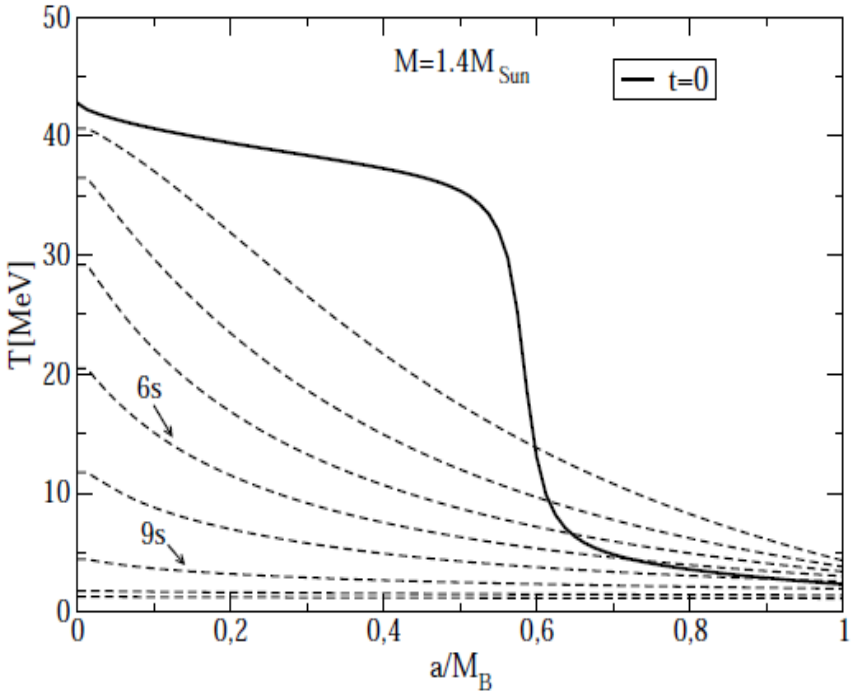

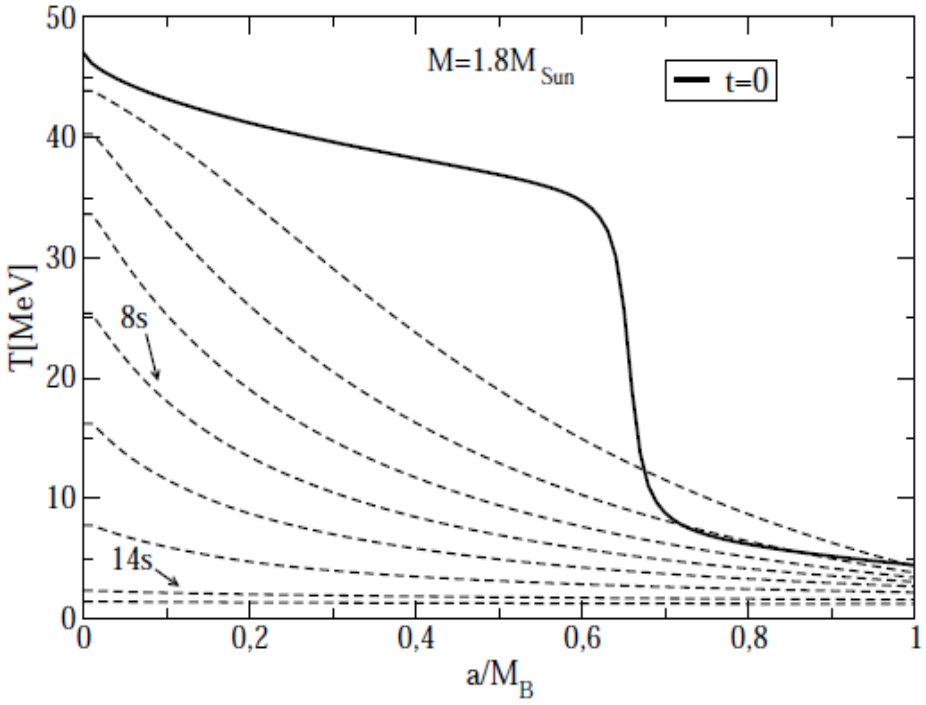

Luminosity curves similar to the protoneutron stars neutrino luminosities. Possible corrections due to lepton number conservation...

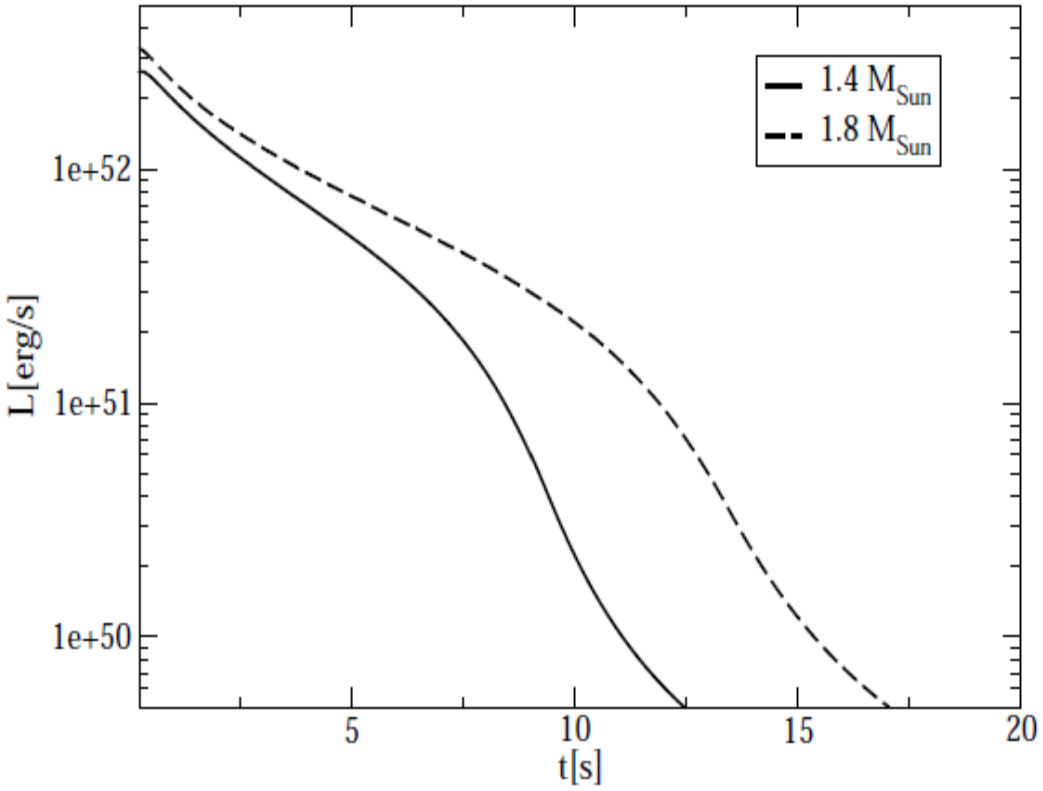

Phenomenology I: such a neutrino signal could be detected for events occurring in our galaxy (possible strong neutrino signal lacking the optical counterpart if the conversion is delayed wrt the SN)

Phenomenology II: connection with double GRBs within the protomagnetar model

UNUSUAL CENTRAL ENGINE ACTIVITY IN THE DOUBLE BURST GRB 110709B

Bin-Bin Zhang[1], David N. Burrows[1], Bing Zhang[2], Peter Mészáros[1,3], Xiang-Yu Wang[4,5], Giulia Stratta[6,7], Valerio D'Elia[6,7], Dmitry Frederiks[8], Sergey Golenetskii[8], Jay R. Cummings[9,10], Jay P. Norris[11], Abraham D. Falcone[1], Scott D. Barthelmy[12], Neil Gehrels[12]

Draft version January 17, 2012

ABSTRACT

The double burst, GRB 110709B, triggered *Swift*/BAT twice at 21:32:39 UT and 21:43:45 UT, respectively, on 9 July 2011. This is the first time we observed a GRB with two BAT triggers. In this paper, we present simultaneous *Swift* and Konus-*WIND* observations of this unusual GRB and its afterglow. If the two events originated from the same physical progenitor, their different time-dependent spectral evolution suggests they must belong to different episodes of the central engine, which may be a magnetar-to-BH accretion system.

Subject headings: gamma-ray burst: general